EXPERIMENTAL INVESTIGATION OF GROUND EFFECTS ON A HEATED CYLINDER IN CROSSFLOW

Jon Philip McComas

NAVAL POSTGRADUATE SCHOOL
Monterey, California

THESIS

EXPERIMENTAL INVESTIGATION OF GROUND
EFFECTS ON A HEATED CYLINDER IN CROSSFLOW

by

Jon Philip McComas

December 1974

Thesis Advisor: T. E. Cooper

Approved for public release; distribution unlimited.

Unclassified

SECURITY CLASSIFICATION OF THIS PAGE (When Data Entered)

REPORT DOCUMENTATION PAGE		READ INSTRUCTIONS BEFORE COMPLETING FORM
1. REPORT NUMBER	2. GOVT ACCESSION NO.	3. RECIPIENT'S CATALOG NUMBER
4. TITLE (and Subtitle) EXPERIMENTAL INVESTIGATION OF GROUND EFFECTS ON A HEATED CYLINDER IN CROSSFLOW		5. TYPE OF REPORT & PERIOD COVERED Master's Thesis; December 1974 6. PERFORMING ORG. REPORT NUMBER
7. AUTHOR(s) Jon Philip McComas		8. CONTRACT OR GRANT NUMBER(s)
9. PERFORMING ORGANIZATION NAME AND ADDRESS Naval Postgraduate School Monterey, California 93940		10. PROGRAM ELEMENT, PROJECT, TASK AREA & WORK UNIT NUMBERS
11. CONTROLLING OFFICE NAME AND ADDRESS Naval Postgraduate School Monterey, California 93940		12. REPORT DATE December 1974 13. NUMBER OF PAGES 67
14. MONITORING AGENCY NAME & ADDRESS(if different from Controlling Office) Naval Postgraduate School Monterey, California 93940		15. SECURITY CLASS. (of this report) Unclassified 15a. DECLASSIFICATION/DOWNGRADING SCHEDULE

16. DISTRIBUTION STATEMENT (of this Report)

Approved for public release; distribution unlimited.

17. DISTRIBUTION STATEMENT (of the abstract entered in Block 20, if different from Report)

18. SUPPLEMENTARY NOTES

19. KEY WORDS (Continue on reverse side if necessary and identify by block number)

Liquid crystals
Forced convection heat transfer
Right circular cylinder heat transfer
constant heat flux cylinder heat transfer
Bluff body heat transfer

20. ABSTRACT (Continue on reverse side if necessary and identify by block number)

The fluid flow and forced convective heat transfer characteristics of a uniformly heated right circular cylinder resting on a flat plate in a cross-flow of air were experimentally investigated.

The circumferential variation of the Nusselt number on the cylinder surface was obtained at Reynolds numbers ranging from 53,000 to 153,000 using a liquid crystal thermographic technique. Pressure coefficients were obtained at five-degree intervals around the cylinder circumference at Reynolds numbers of 105,000 and 156,000. Flow visualization was conducted at a Reynolds number of

DD FORM 1 JAN 73 1473 (Page 1) EDITION OF 1 NOV 63 IS OBSOLETE S/N 0102-014-6601

Unclassified

SECURITY CLASSIFICATION OF THIS PAGE (When Data Entered)

Block 19. Key Words (Cont.)

Heat transfer from a cylinder resting on a flat plate
Proximity effects
Local heat transfer coefficients around a cylinder
Incompressible flow around a cylinder

Block 20. Abstract (Cont.)

10,000 in order to qualitatively examine the flow field.

A qualitative theory based upon a compilation of previous results reported for flow around a "free" cylinder and flow over forward and rear-facing steps was developed.

Experimental results obtained were in agreement with the proposed theory, and heat transfer and pressure data correlated well with one another. In the region between 0 and 180 degrees, the heat transfer and pressure results correlated quantitatively with the results obtained by Meyer for a "free" cylinder at Reynolds numbers above 300,000.

Experimental Investigation of Ground Effects on a Heated Cylinder in Crossflow

by

Jon Philip McComas
Lieutenant, United States Navy
B.S., United States Naval Academy, 1967

Submitted in partial fulfillment of the
requirements for the degree of

MASTER OF SCIENCE IN MECHANICAL ENGINEERING

from the

NAVAL POSTGRADUATE SCHOOL
December 1974

ABSTRACT

The fluid flow and forced convective heat transfer characteristics of a uniformly heated right circular cylinder resting on a flat plate in a crossflow of air were experimentally investigated.

The circumferential variation of the Nusselt number on the cylinder surface was obtained at Reynolds numbers ranging from 53,000 to 153,000 using a liquid crystal thermographic technique. Pressure coefficients were obtained at five-degree intervals around the cylinder circumference at Reynolds numbers of 105,000 and 156,000. Flow visualization was conducted at a Reynolds number of 10,000 in order to qualitatively examine the flow field.

A qualitative theory based upon a compilation of previous results reported for flow around a "free" cylinder and flow over forward and rear-facing steps was developed.

Experimental results obtained were in agreement with the proposed theory, and heat transfer and pressure data correlated well with one another. In the region between 0 and 180 degrees, the heat transfer and pressure results correlated quantitatively with the results obtained by Meyer for a "free" cylinder at Reynolds numbers above 300,000.

TABLE OF CONTENTS

LIST OF ILLUSTRATIONS

Figure

ACKNOWLEDGEMENT

I would like to express my sincere appreciation to the following persons who were especially helpful to me during the conduct of this investigation:

Mr. Jack McKay, Mr. George Bixler, and Mr. Thomas Christian, who contributed their technical expertise to the construction and modification of the experimental apparatus;

Mr. Bob Besel, Mr. Ted Dunton, and Mr. Stan Johnson, who assisted me in the scheduling, set-up, and operation of the wind tunnel;

Professor Matthew Kelleher and Professor T. Sarpkaya, who provided me with many helpful suggestions for both the conduct and reporting of this work.

I would also like to offer special thanks to my advisor, Professor Thomas Cooper, for the encouragement and guidance he provided througnout this work and for the faith he showed in me.

Finally, I wish to thank my wife for the patience and understanding she offered throughout the course of this project.

I. INTRODUCTION

The primary purpose of this work was to investigate the forced convective heat transfer and fluid flow characteristics of a uniformly heated right circular cylinder resting on a flat plate in a crossflow of air. This particular flow situation models several situations of practical interest, notably, the effect of wind on rocket motor storage containers lying on the ground. In this regard, this investigation supports the previous work reported by Wirzburger [1]*.

Local Nusselt numbers were obtained at various circumferential locations on the cylinder for Reynolds numbers in the range of 53,000 to 153,000 using the liquid crystal technique developed by Field [2]. A four-inch diameter cylinder was rigidly attached to a flat plate and placed in a low speed wind tunnel with a turbulence intensity of approximately 0.5 to 0.7 percent. The test cylinder was constructed of a carbon-impregnated resistive paper having an electrical resistivity of approximately one ohm-inch. The cylinder was coated with microencapsulated cholesteric liquid crystals and packed inside with glass wool for the purposes of both minimizing conduction and internal free convection losses, and providing resistance to deformation. The cylinder surface was uniformly heated by passing an electrical current through the resistive paper, and data were obtained by observing the position of the isotherms indicated by the liquid crystals.

Pressure coefficients were also obtained on the surface of the cylinder. A rotatable four-inch diameter aluminum cylinder was fitted with four 0.025 inch static pressure taps 90 degrees apart. The cylinder was sealed to the flat plate by means of a Teflon strip which allowed the cylinder to

*Numbers in brackets refer to references at end of thesis.

rotate, but did not allow flow to pass between the plate and the cylinder. Pressure data were obtained using a manometer bank referenced against atmospheric pressure. Stagnation pressure and test section static pressure were obtained from existing pressure taps in the wind tunnel which were connected to the same manometer bank.

Flow visualization was conducted in a water tunnel using a 1.5-inch diameter plexiglas cylinder sealed against an aluminum flat plate. The system was scaled for dynamic similitude with the heat transfer experimental apparatus. The cylinder was equipped with three dye ports, two of which were located approximately 30 degrees either side of the attachment point, and the other located at approximately the 90 degree mark. Due to limitations in the water pump, the maximum Reynolds number which could be attained with this apparatus was approximately 10,000.

A qualitative theory of the flow field and accompanying heat transfer was proposed based upon previous investigations of flow around a "free" cylinder combined with investigations of flow over forward and rear-facing steps.

The heat transfer and pressure data obtained were in excellent agreement with the proposed theory, and the pressure data correlated well with the heat transfer data. The flow visualization showed agreement with portions of the proposed theory, but did not support the heat transfer and pressure data on certain regions of the cylinder. This is most probably because of the wide difference in the Reynolds number between these experiments.

II. THEORY

A thorough search of the existing literature indicated that this particular flow situation had not been examined. The study of flow around a "free" cylinder has been studied extensively, and an excellent bibliography on the subject has been presented by Meyer [3]. Subsequent to Meyer's work, Field [2] investigated both subcritical and critical flow around a right circular cylinder in crossflow using the liquid crystal technique employed in this investigation. A brief description of these two flow situations is presented below.

In subcritical flow, a laminar boundary layer develops at the forward stagnation point of the cylinder and grows to a maximum thickness at an angular location of 80 to 85 degrees. Concurrently, the heat transfer coefficient decreases as the boundary layer thickness increases in this region. At 80 to 85 degrees, the kinetic energy of the moving fluid is no longer sufficient to overcome the adverse pressure gradient present on the cylinder's surface, and the laminar boundary layer separates. Upon separation, a wake is formed in the rear portion of the cylinder, and the turbulent action in the wake tends to circulate cooler fluid to the surface of the cylinder. As a result of this action, the heat transfer coefficient increases in this area.

In critical flow, which occurs at Reynolds numbers above approximately 120,000, the laminar boundary layer again grows from the forward stagnation point to the 80 to 85 degree point where separation again occurs. However, in this case the kinetic energy of the fluid is enough to overcome the adverse pressure gradient, and the flow reattaches itself to the cylinder

surface at a point approximately 15 degrees aft of the laminar separation point. This separation "bubble" is [illegible] by highly turbulent mixing and results in a sudden increase in heat transfer. From the point of reattachment, a turbulent boundary layer begins to grow to a point in the region of 110 to 130 degrees where it separates. The heat transfer coefficient decreases as the turbulent boundary layer thickens. Upon separation of the turbulent boundary layer, the action of the wake causes an increase in the heat transfer coefficient.

It should be noted that the above description is confined to a right circular cylinder which is freely suspended in crossflow such that flow can pass over both sides. Hence, the flow pattern is spacially symmetrical. There was no reason to expect this to be the case in this investigation, however, and an attempt was made to gain some understanding of what results might be expected in the regions of the cylinder near the flat plate. This was accomplished by examining the cases of flow over forward-facing and rear-facing steps.

The problem of flow over forward-facing and rear-facing steps has been examined in various lights. Several investigators have focused on the determination of the location of the separation points and reattachment points [4-9]. Others have examined the heat transfer and pressure distribution within the separated regions [10-17]. However, these investigations were primarily concerned with the regions of the flat plate either forward or aft of the step and did not deal with the step itself. Since a cylinder resting on flat surface represents a type of "step", this region was of most interest in this work. A few investigators did conduct flow visualization experiments in conjunction with their other goals, however, and their results proved to be of benefit in predicting the nature of the flow in the regions of the cylinder near the flat plate.

Of particular interest were the findings of Abbott and Kline [5] for rear-facing steps, and those of Luzhanskii and Emtsev [10] for forward-facing steps. The latter investigated the zone of turbulent boundary layer separation ahead of a forward-facing step at Reynolds numbers of 17,000 to 420,000 based upon step height. Although their visualization technique was not described, their experiments were conducted in air. The results of this investigation are shown in Figure 1. It should be noted that, in addition to the normal separation vortex (points 1-2-1), another small "trapped" vortex was noted in the region between points 3 and 4.

Abbott and Kline conducted flow visualization experiments using the dye injection method on a variable height backward-facing step placed in a water tunnel. The boundary layer at separation from the step was turbulent as is the case for critical flow around a cylinder. The experiments were conducted in a Reynolds number range of 20,000 to 50,000 based upon the height of the water channel above the step. Their results indicated that three regions of flow existed downstream of the step. Region I was characterized by one or more vortices rotating about an axis normal to the vertical wall and parallel to the floor. These vortices were three-dimensional in nature, and adjacent vortices were counter-rotating and not necessarily the same size. Region II contained the classical pattern of separation, i.e. flow moving two-dimensionally upstream next to the wall and downstream adjacent to the through flow. Region III was of no interest to the present investigation because it did not directly affect the step. The three regions are depicted both in plan and elevation views in Figure 2.

From a compilation of the results described above and those observed for a "free" cylinder, the following theory was developed.

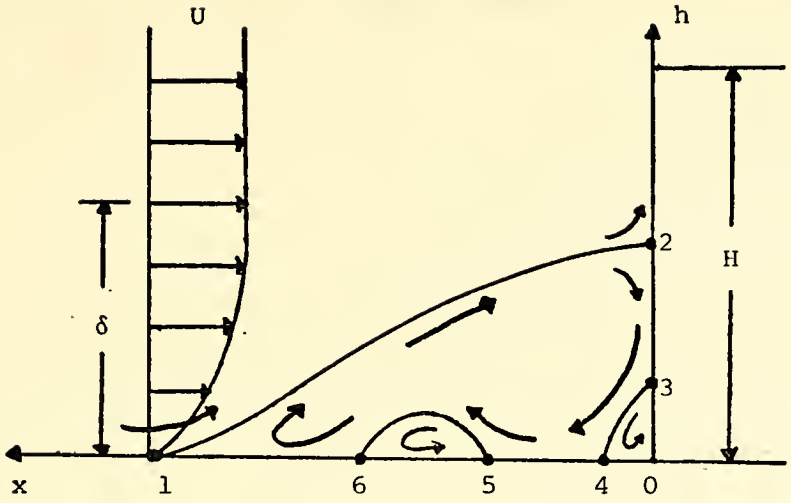

Figure 1. Flow pattern ahead of a step as observed by Luzhanskiy and Solntsev.

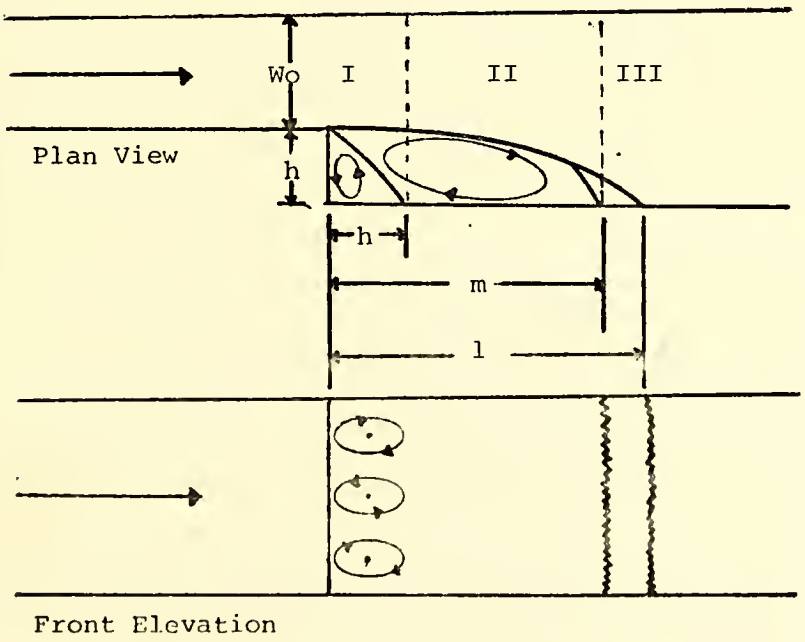

Figure 2. Flow pattern at the rear of a step as observed by Abbott and Kline.

As the flow proceeds along the flat plate, a boundary layer will develop and grow on the plate until, at some point upstream of the cylinder, this boundary layer will separate. At the flow velocities to be used in the experimental portion of this investigation, this boundary layer can be anticipated to be laminar. From this point, it is theorized that the flow will be characterized by a behavior similar to that observed by Luzhanskiy and Solntsev, i.e. a portion of the flow will reattach to the cylinder at some point on the forward portion of its circumference, and the remainder of the flow will assume the classical separation pattern with the addition of a system of "trapped" vorticies near the intersection of the cylinder and the flat plate. The flow which reattaches itself to the cylinder then will assume the classical pattern described previously for flow around a "free" cylinder, with the differentiation between subcritical and critical flow being dependent upon the Reynolds number. Regardless of whether the flow is subcritical or critical, it will separate. Upon separation, it is assumed that a pattern similar to that observed by Abbott and Kline will be present.

From the above theory of the flow phenomenon, the heat transfer results can be predicted. For ease of explanation the cylinder will be described as consisting of three regions. Region I consists of that portion of the cylinder circumference between the point of attachment of the cylinder to the flat plate and the point at which the separated flow from the plate reattaches to the cylinder. This latter point will hereafter be referred to as the stagnation point for simplicity. Region II consists of that portion of the cylinder circumference between the stagnation point and the point of final boundary layer separation. Region III consists of that portion of the cylinder circumference aft of the final separation point.

The phenomenon which is proposed to occur in Region I is depicted in Figure 3. Since all the fluid within the separation zone is "trapped," heat liberated from the cylinder surface must be conducted from vortex to vortex within the separation region and ultimately conducted to the free stream through the free shear layer separating the separation zone from the free stream. This being the case, the bulk temperature in the larger vortices must be less than the bulk temperature in the smaller vortices in order for a driving potential for conduction to exist. Convection, however, also plays a role in this process in that a redistribution of energy within individual vortices is accomplished by convection. It is assumed that the vortices will become smaller and weaker as the attachment point is approached such that, very near this point, the heat transfer will approach a pure conduction case. Hence, the resistance to heat transfer should increase from the stagnation point to the attachment point. If the thermal resistance increases, the wall temperature must also increase in order to insure that a constant heat flux is transferred to the fluid. If the wall temperature increases and the free stream temperature and surface heat flux remain constant, the heat transfer coefficient must decrease. Hence, in the absence of other effects, the heat transfer coefficient should decrease from a relative maximum at the stagnation point to a zero value at the attachment point (assuming the flat plate is adiabatic). Superimposed upon on this phenomenon, however, is the behavior of the heat transfer coefficient near the intersection of two vortices. The region between points 1 and 3 of Figure 3 is illustrative of this behavior. At point 1, the stagnation point, the fluid in the vortex which impacts on the cylinder surface is relatively cool because some of its energy has just been conducted to the free stream. As the fluid proceeds toward

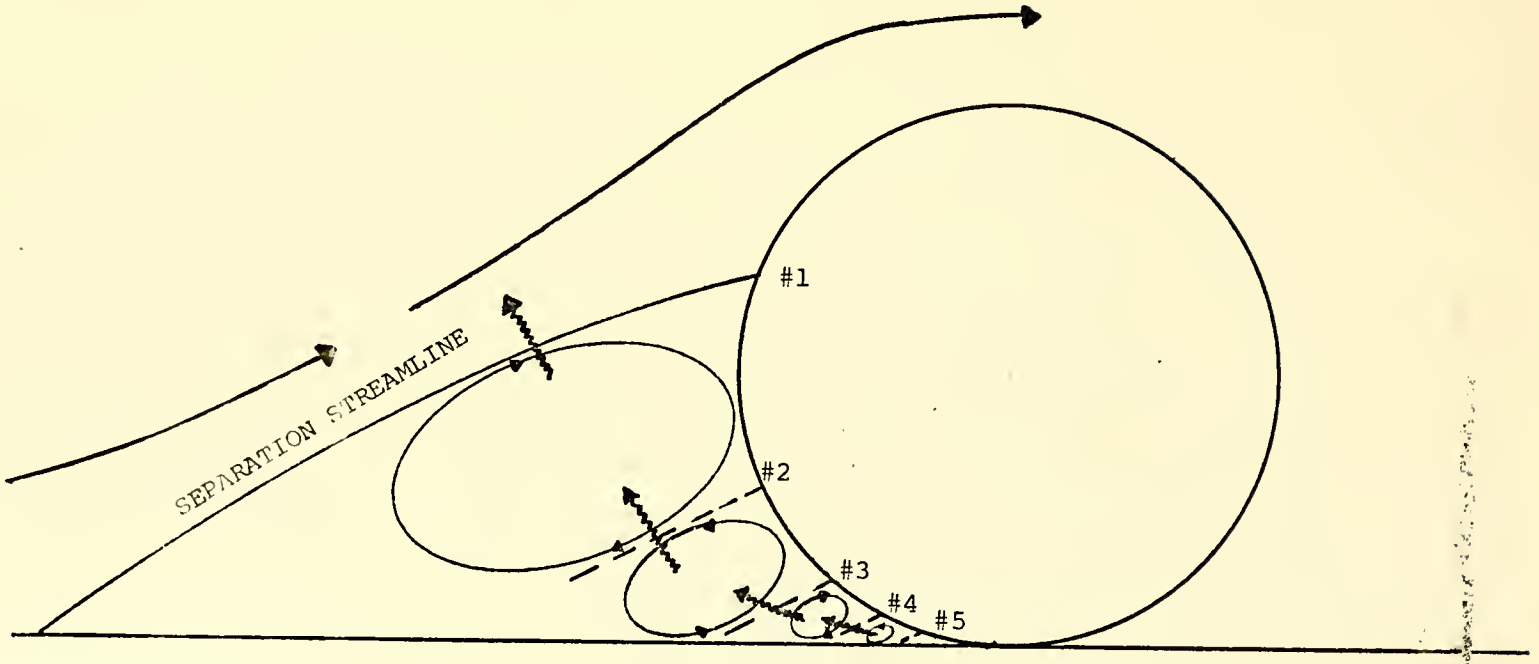

Figure 3. Region I of the cylinder resting on a flat plate.

point 2, it is heated and its thermal resistance is increased; hence, the heat transfer coefficient is decreased in this region. Since adjacent vortices are counter-rotating, a similar behavior should occur between points 3 and 2. Therefore, point 2 should appear as a relative minimum in the heat transfer coefficient, and the heat transfer coefficient should then increase to a relative maximum at point 3. At point 3, the cycle described above should begin again, this time involving points 3, 4, and 5. It should be noted that, because the vortices become smaller and weaker as the point of attachment is approached, this secondary effect may become experimentally imperceptible in the region near this point. It should also be noted that the number of vortices depicted in the schematic does not consititute a prediction of how many will actually be present.

Region II is characterized by the results reported by Field [2] for subcritical or critical flow, whichever may be the case.

Region III is theorized to indicate an initial increase in the heat transfer coefficient due to the turbulent action of the wake. However, at some point, this increase will be overridden by the phenomenon described for Region I, and the heat transfer coefficient will decrease to a zero value at the attachment point.

Schematics depicting the theorized flow situation and accompanying heat transfer data for both subcritical and critical flows are shown as Figures 4 and 5 respectively. The locations at which various phenomenon occur are conjectural and should not be construed as being exact predicted values.

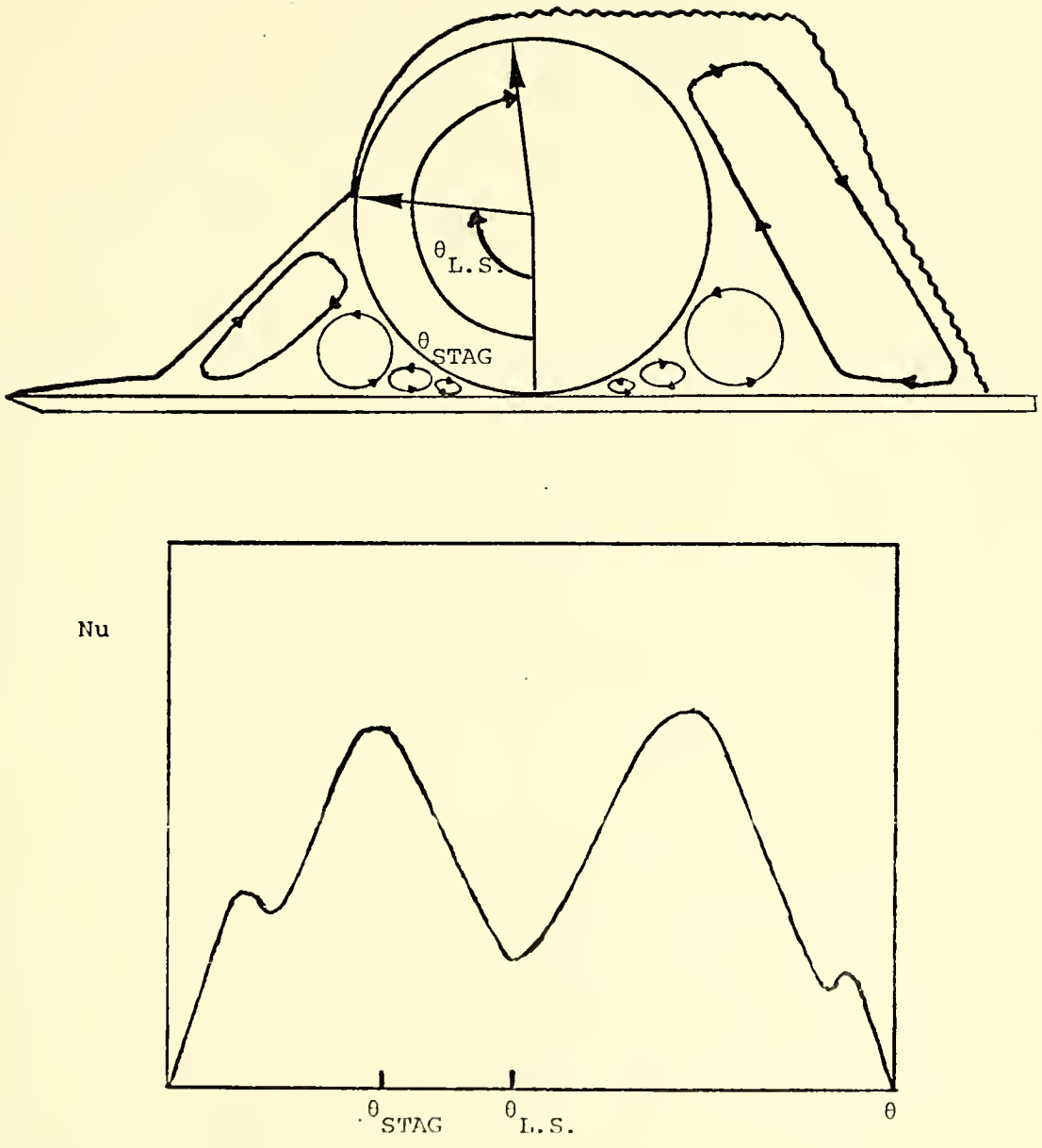

Figure 4. Proposed flow pattern for subcritical Reynolds numbers.

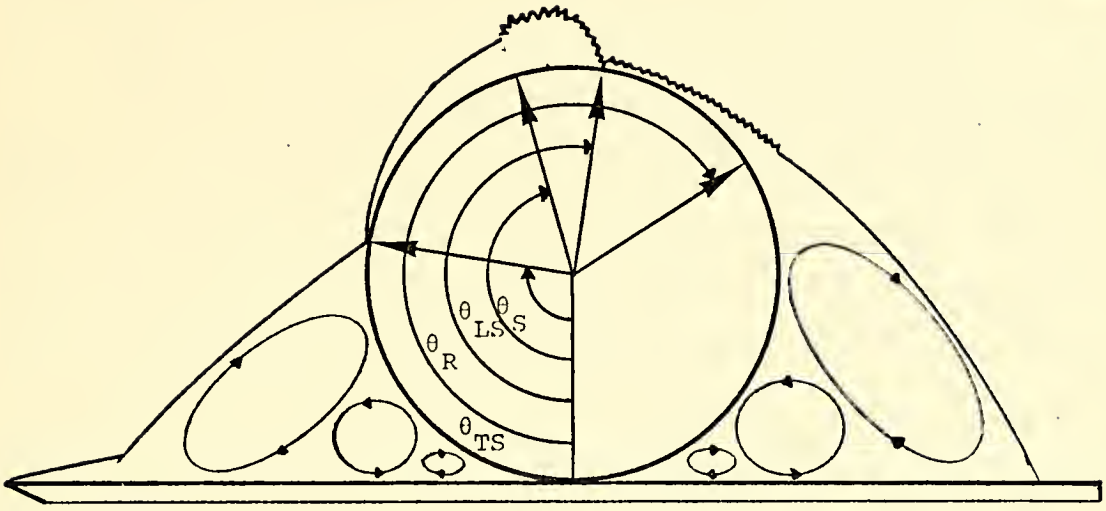

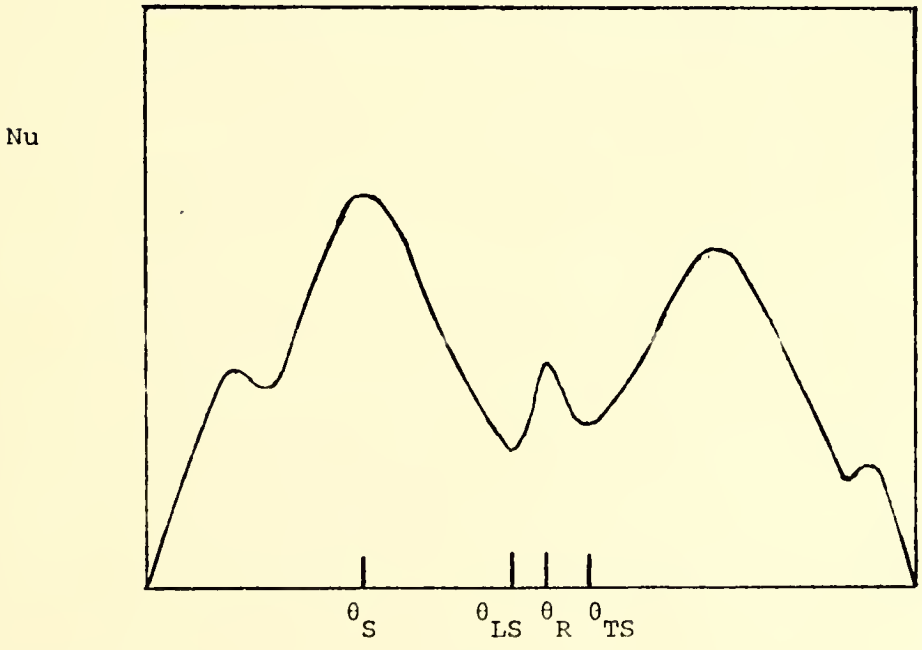

Figure 5. Proposed flow pattern for critical Reynolds numbers.

III. EXPERIMENTAL APPARATUS

A. HEAT TRANSFER EXPERIMENT

1. Liquid Crystals

Microencapsulated cholesteric liquid crystals were used in this investigation. This substance, when applied to a dark background, provides a visual display of temperature by means of a change of color. The surface coated with liquid crystals traverses the visible color spectrum within a certain temperature band with an accuracy of approximately $0.2^{\circ}F$. The size of this band is determined by the formulation of the cholesterol esters in the mixture. Only one liquid crystal formulation was used in this investigation, NCR designation S-43. The batch used had been calibrated previously by Field [2], and the results of this calibration indicated that liquid crystal S-43 transitioned to a red color at $109.8^{\circ}F$, to a green color at $111.0^{\circ}F$, and to a blue color at $112.3^{\circ}F$. An excellent list of references on the theory and use of liquid crystals can be found in Field's work.

2. Cylinder Design and Construction

The cylinder utilized in the collection of heat transfer data was similar in design to that used by Field. The actual working section was constructed from a 12-inch square sheet of Armstrong Temsheet, a carbon-impregnated, electrically resistive paper having an electrical resistance of approximately 25 ohms per square and a nominal thickness of 0.039 inches. The heat generated when a constant current is passed through the paper is uniform to within two percent from point to point over a large area. This sheet was fashioned into a cylinder having an outside diameter of 4.03 inches and a height of 12 inches.

Aluminum conducting tape was applied as electrodes circumferentially on the inner surface of this cylinder to insure uniform application of voltage. These electrodes were located three inches from the top and bottom of the cylinder in order that edge conduction effects would be eliminated. This established a six inch height of cylinder in which data would be taken. Silver conducting paint was applied to the interface between the tape and the paper to insure intimate electrical contact was maintained between the two surfaces.

The base assembly consisted of two 4.03-inch diameter wooden cylinders, each 14.75 inches long, rigidly attached to each other by an eight-inch long wooden bar. The outside surface of this bar was of the same curvature as the cylinders in order to insure that no discontinuities existed near the point of attachment to the flat plate. The purpose of this bar was to maintain alignment between the two base cylinders, and to allow the Temsheet cylinder to be taped along its length to the bar. The entire assembly was slotted to accept a 1/4-inch square plexiglas rod along its length. This rod accepted screws from the flat plate to insure that an acceptable seal was maintained at the point of attachment. The base assembly is shown in Figure 6.

Each base cylinder was of sufficient length such that it would extend through the floor/ceiling of the wind tunnel where it could be clamped thus providing added rigidity to the assembly. The other ends of the base cylinders were turned down approximately 0.04 inches over a two-inch length. This allowed the paper to be attached to the bases with double-backed tape and present a constant diameter of 4.03 inches along the entire length of the assembly. The bottom base was drilled through its axis with a one-inch diameter hole through which the electrical leads

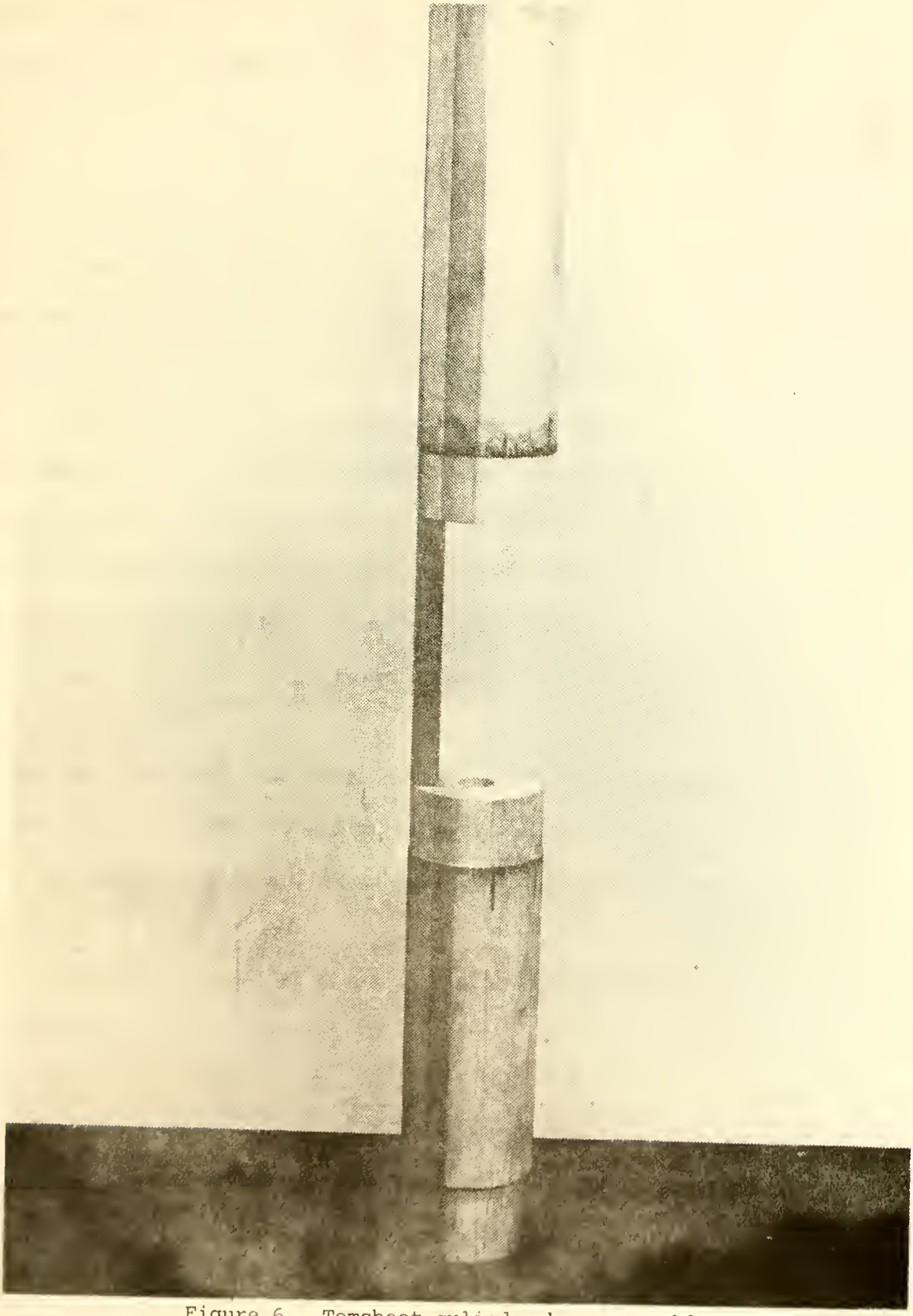

Figure 6. Temsheet cylinder base assembly.

could be passed to the power supply; and the top base was drilled through its axis with a two-inch diameter hole to provide a means of filling the Temsheet cylinder with glass wool. The glass wool served the dual purpose of providing insulation against possible internal heat losses due to conduction or natural convection and of providing the paper cylinder with added resistance to deformation.

Two coats of slurry-based liquid crystal S-43 were applied to the Temsheet cylinder, and it was marked at five-degree intervals for accurate location of the liquid crystal isotherms during the experiment.

The flat plate was constructed from a sheet of 1/2-inch plexiglas and was 36 inches long and 32 inches high. Plexiglas was selected for this construction in order that the entire circumference of the cylinder could be viewed from outside the wind tunnel. The leading edge of the plate was beveled approximately 14 degrees to insure that a sharp leading edge was presented to the flow. The point of attachment of the cylinder was located on a vertical line 18 inches downstream of the leading edge. At this point, the plate was notched along its height to accept the plexiglas rod on the cylinder assembly, and attachment was accomplished by four screws. This design insured that flow could not pass between the cylinder and the plate.

The wind tunnel in which this cylinder assembly was placed was the low speed Aerolab wind tunnel located in the Aeronautics Laboratory in Halligan Hall, U. S. Naval Postgraduate School. This tunnel is powered by a 100 hp electric motor and is capable of producing wind velocities of up to 200 mph with a clear test section. The tunnel has a turbulence level as measured by hot wire anemometer of approximately 0.5 to 0.7 percent. A schematic of the wind tunnel with pertinent dimensions is shown in Figure 7.

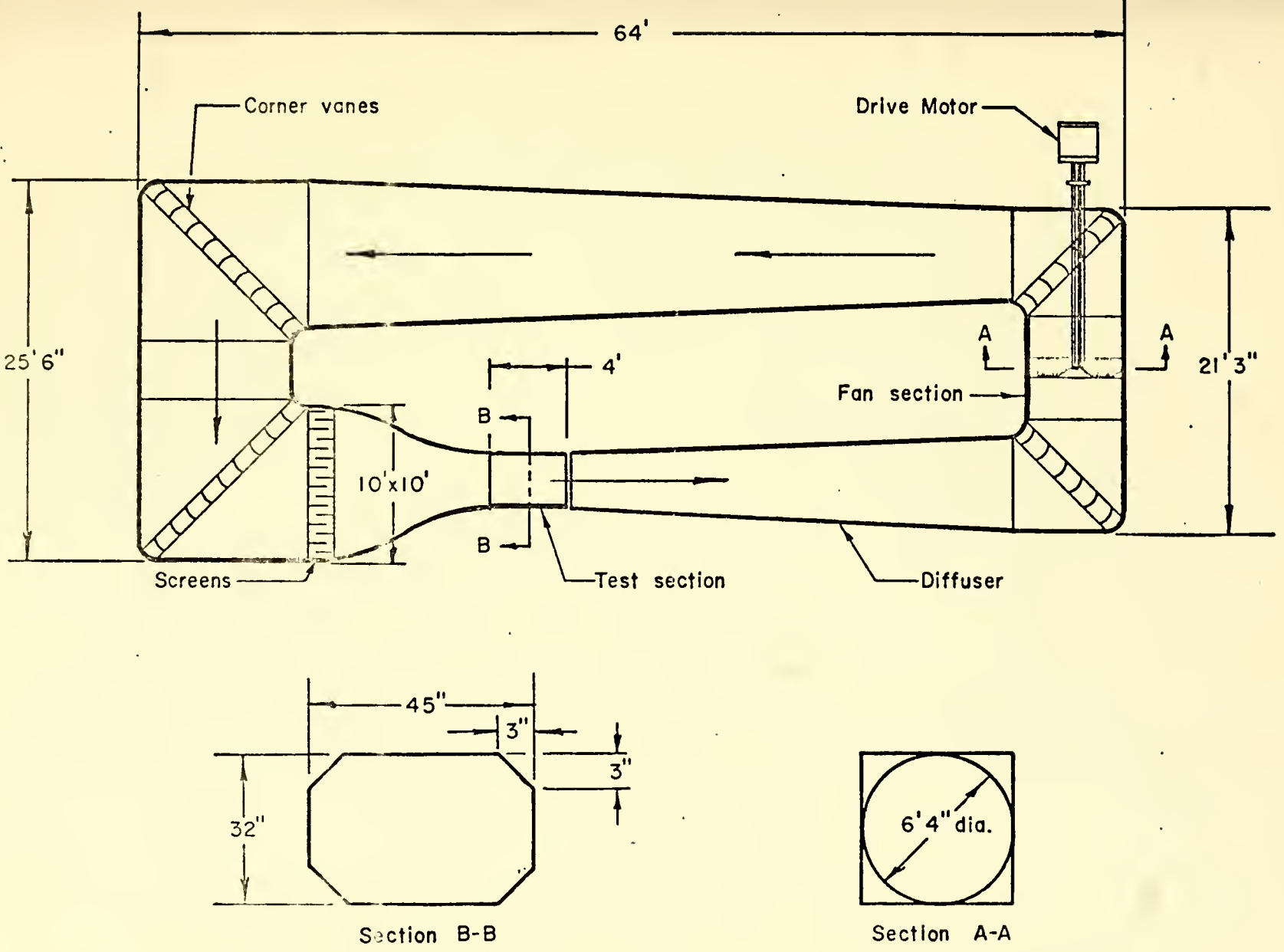

Figure 7. Schematic diagram of the wind tunnel.

The combined cylinder and plate assembly was located in the wind tunnel test section such that the longitudinal axis of the flat plate lay along a line eight inches from one wall of the test section. By off-centering the assembly in this manner, the effects of the flow along the wind tunnel wall on the cylinder were effectively eliminated.

B. PRESSURE EXPERIMENT

In order to obtain static pressure measurements of this particular flow situation, a 4.03-inch diameter cylinder was constructed of aluminum. This cylinder was fitted with four 0.025-inch surface pressure taps spaced at 90-degree intervals around the circumference of the cylinder at approximately mid-height of the wind tunnel test section. In order that this cylinder could be rotated and a seal still be maintained, a Teflon strip was inserted into the notch in the flat plate described previously. This strip provided for a snug fit between the cylinder and the plate, and the flexibility of the Teflon allowed for relatively easy rotation. The cylinder was scribed as five-degree intervals about its circumference at the point where it intersected the wind tunnel test section floor. Reference lines were scribed on the floor at 90-degree intervals so that the matching of the scribe marks on the cylinder with these lines provided a means of accurately establishing the angular location of the pressure taps. The pressure cylinder is shown in Figure 8.

The surface pressure taps were connected to a water manometer bank by means of plastic tubing. The monometer bank was referenced against atmospheric pressure. Wind tunnel plenum chamber static pressure and test section static pressure were measured on the same manometer bank through pre-existing connections on the wind tunnel.

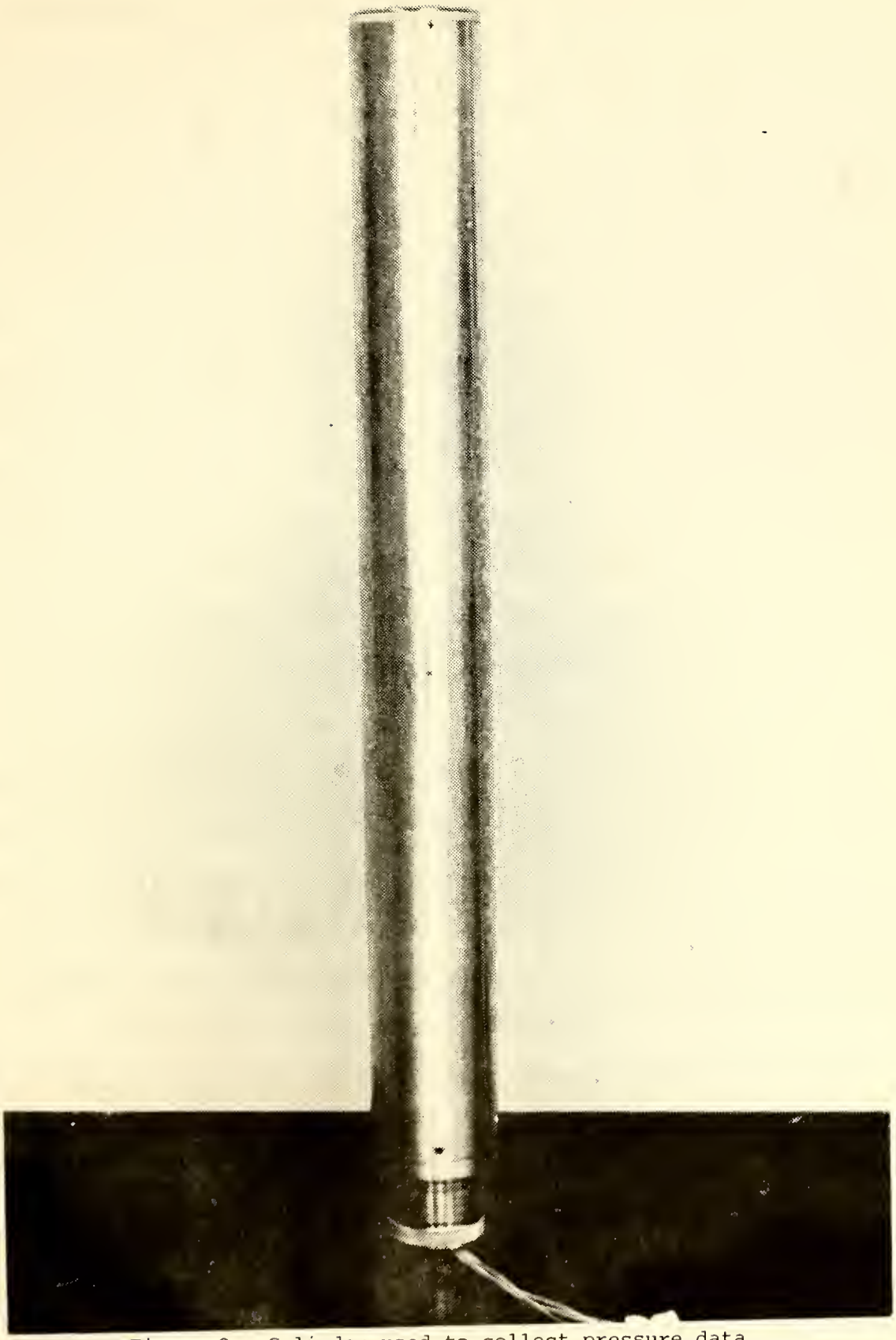

Figure 8. Cylinder used to collect pressure data.

C. FLOW VISUALIZATION EXPERIMENT

The apparatus used for flow visualization consisted of a converging wooden water channel 15 feet in length and 13 inches deep with a plexiglas test section 13 inches long, 12 inches wide, and 13 inches deep. A hollow, 1.5-inch diameter plexiglas cylinder was attached between the test section walls with its longitudinal axis located eight inches from the test section floor. In order to preserve dynamic similitude, a 1/4-inch thick steel flat plate was constructed to the scale of the ratio of the water tunnel cylinder diameter to the wind tunnel cylinder diameter (0.375:1). Thus, this plate was 13.5 inches long and 12 inches wide. The leading edge was beveled to a 14 degree angle as was the larger flat plate used in the wind tunnel. The flat plate was placed atop the cylinder, and the point of attachment was sealed by a layer of tape. The cylinder was fitted with three dye ports which were connected by rubber tubing to three separate dye reservoirs with individual valving located approximately three feet higher than the cylinder. This additional height insured that a constant head was maintained on the injection system, and the individual valving was necessary to allow each port to be operated separately in order that the flow field at various sections of the cylinder could be observed independently.

Water was pumped into the channel by means of an irrigation pump directly coupled to a Westinghouse Type SK dynamometer running as a motor. With the motor running at 1500 RPM, the pump output was approximately 1000 gallons per minute. The depth of water in the channel was controlled by a tilting weir at the end of the channel. For this particular experiment, the water depth was maintained at 10 inches. This allowed the entire apparatus to be immersed to a minimum depth in order that free surface effects could be minimized.

IV. EXPERIMENTAL PROCEDURES

A. HEAT TRANSFER EXPERIMENT

Prior to conducting the experiment, the thermocouple used to measure airstream temperature and its ice bath reference junction were examined, and the micromanometer used to measure wind velocity was leveled and carefully zeroed. The test cylinder power leads were then connected to a Weston ohmmeter, and the cylinder resistance was determined. The leads were then switched to a Lambda regulated power supply model LK345A, and voltage was applied until the temperature of the entire cylinder surface fell within the event temperature range of liquid crystal S-43 causing the cylinder to undergo a color change. This procedure was necessary to insure that the glass wool packing was adjusted properly so that regions of temperature discontinuity did not exist. The wind tunnel was then started and brought to a predetermined velocity at which it was maintained throughout the run. Applied voltage was adjusted until distinct positions of temperature transition could be observed. After steady state was reached, the angular locations and magnitudes of these isotherms were recorded in addition to the values of applied voltage and airstream temperature. A steady state condition was usually attained in from five to ten minutes dependent upon the wind velocity. The voltage was then changed until the angular location of the isotherms had changed a significant amount, and data were recorded again. This process was repeated until isotherms had been observed at reasonable intervals around the circumference of the cylinder. Through this procedure, a plot of local Nusselt number versus angular location could be quickly and easily obtained.

Runs were made at nine Reynolds numbers ranging between 53,000 and 153,000. Each run was accomplished in from 60 to 90 minutes, this time being dependent upon Reynolds number. For all runs the points of temperature transition were easily distinguishable around the entire circumference of the cylinder except in the region from 0 to 45 degrees and in the region from 180 to 210 degrees. In these regions, the temperature gradient was very shallow, and the entire region appeared isothermal. In addition, data were not obtainable in the regions 15 degrees either side of the attachment point (the 270 degree mark) because a break in the resistive paper was necessary in these regions to facilitate the attachment of the cylinder to the flat plate.

B. PRESSURE EXPERIMENT

Pressure data were obtained at Reynolds numbers of 105,000 and 156,000. Initially, the manometer bank was leveled, all leads were checked for tightness, and the air temperature was recorded for evaluation of transport properties. The pressure taps were initially located at 0, 90, 180, and 270 degrees. The wind tunnel was started, and the velocity was increased to a predetermined value. Values were recorded for each pressure tap on the cylinder, the wind tunnel plenum chamber static pressure, the test section static pressure, and atmospheric pressure. The cylinder was then rotated in five-degree increments, with data being recorded at each increment, until the entire circumference of the cylinder had been traversed. Data were then reduced, and a preliminary plot of pressure coefficient versus angular location was made. This plot was examined, and regions warranting closer investigation were identified. Data were then obtained at 2 1/2-degree increments within these regions.

C. FLOW VISUALIZATION EXPERIMENT

The motor was started and brought up to a speed of 1500 RPM. The tilting weir was adjusted such that the height of the water in the channel was 10 inches, and the flow was allowed to steady out. The dye was then injected through the existing ports in a trial and error fashion until the flow could be visualized clearly. Most regions of interest could be observed in this manner. In those regions which required closer observation, dye was injected directly into the flow by means of a hypodermic needle.

It became necessary to interrupt the procedure periodically due to the presence of large air bubbles which coalesced on the flat plate downstream of the cylinder. These bubbles were thought to have been caused by entrained air in the water which left solution in regions of low pressure. These bubbles were swept away by hand before the experiment was continued. It should be noted that the effect of these air bubbles was not completely deleterious. In certain regions on the cylinder surface where the dye did not provide adequate information regarding the existing flow conditions, the bubbles could be used as a flow visualization aid. The location of the laminar separation point was found in this manner.

V. RESULTS

A. HEAT TRANSFER EXPERIMENT

Raw data and sample calculations from the heat transfer experiments are contained in Appendix A. This section contains graphical results and comparisons of the local Nusselt number versus angular location for various Reynolds numbers, and of the average Nusselt number versus Reynolds number.

Figure 9 shows the results of the heat transfer experiment for Reynolds numbers of 53,000, 103,500, and 153,000. The ratio of boundary layer thickness on the flat plate to cylinder diameter was approximately 0.3. Since the shape of these curves did not vary throughout the Reynolds number range tested, the curves presented are considered representative. There are several points of interest to be noted from these curves.

First, the flow around the cylinder exhibited critical behavior at all Reynolds numbers tested. Otherwise, there was good agreement between these results and the proposed theory. The stagnation point was located in the region between 5 and 20 degrees and appeared to move toward 0 degrees with increasing Reynolds number. The point of laminar separation was relatively stationary at approximately 75 degrees. Reattachment occurred consistently at approximately 92 degrees, and final separation occurred consistently at approximately 140 degrees. As Reynolds number increased, the point of maximum heat transfer shifted from the stagnation point to the point of reattachment of the turbulent boundary layer. Of particular note are the two points of relative maxima located at approximately 240 and 300 degrees respectively. Since the point of attachment of the cylinder to the flat plate was taken to be the 270 degree mark, these

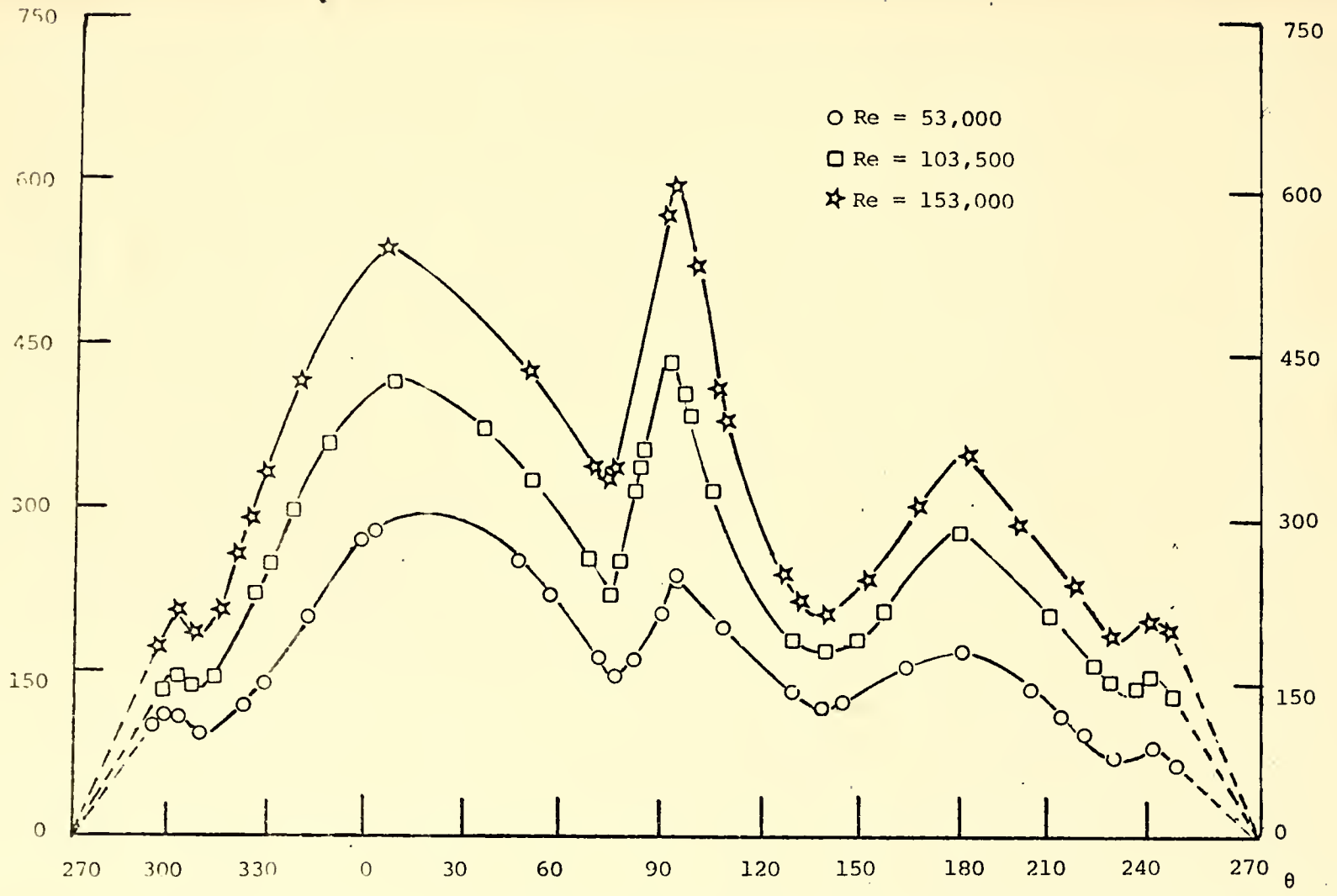

Figure 9. Heat transfer results at Reynolds numbers of 53,000, 103,500, and 153,000.

points lie in the regions in which this type of behavior was postulated by theory.

Figures 10 and 11 are a comparison of the heat transfer data obtained in this investigation with that obtained by Field [2] at two nearly equal Reynolds numbers, one in the subcritical range and one in the critical range. Figure 11 also contains a plot of the data obtained by Meyer [3] at a Reynolds number of 495,000. Additionally, a comparison of average Nusselt number versus Reynolds number for this investigation and Field's investigation is shown as Figure 12. The average Nusselt number was computed from the formula

$$\overline{Nu} = \frac{1}{2\pi} \int_0^{2\pi} Nu \, d\theta$$

which was numerically integrated by computer using Simpson's Rule of Quadrature with a step size of 5 degrees.

It is readily apparent that the presence of the flat plate radically altered the local heat transfer coefficient around the cylinder especially in the classical subcritical Reynolds number range (Reynolds number less than 120,000). In the critical Reynolds number range, the overall trend in the curves was similar, but the comparative values of the Nusselt number at locations of interest were widely differing. In the region from 0 to 120 degrees, the values found in this investigation for Reynolds numbers in the range between 53,000 and 153,000 were on the order of those found by Meyer for a "free" cylinder at Reynolds numbers above 300,000. Field's point of maximum heat transfer occurred at the 180 degree mark whereas, this investigation showed the maximum value to occur at the point of reattachment of the turbulent boundary layer. Meyer also found

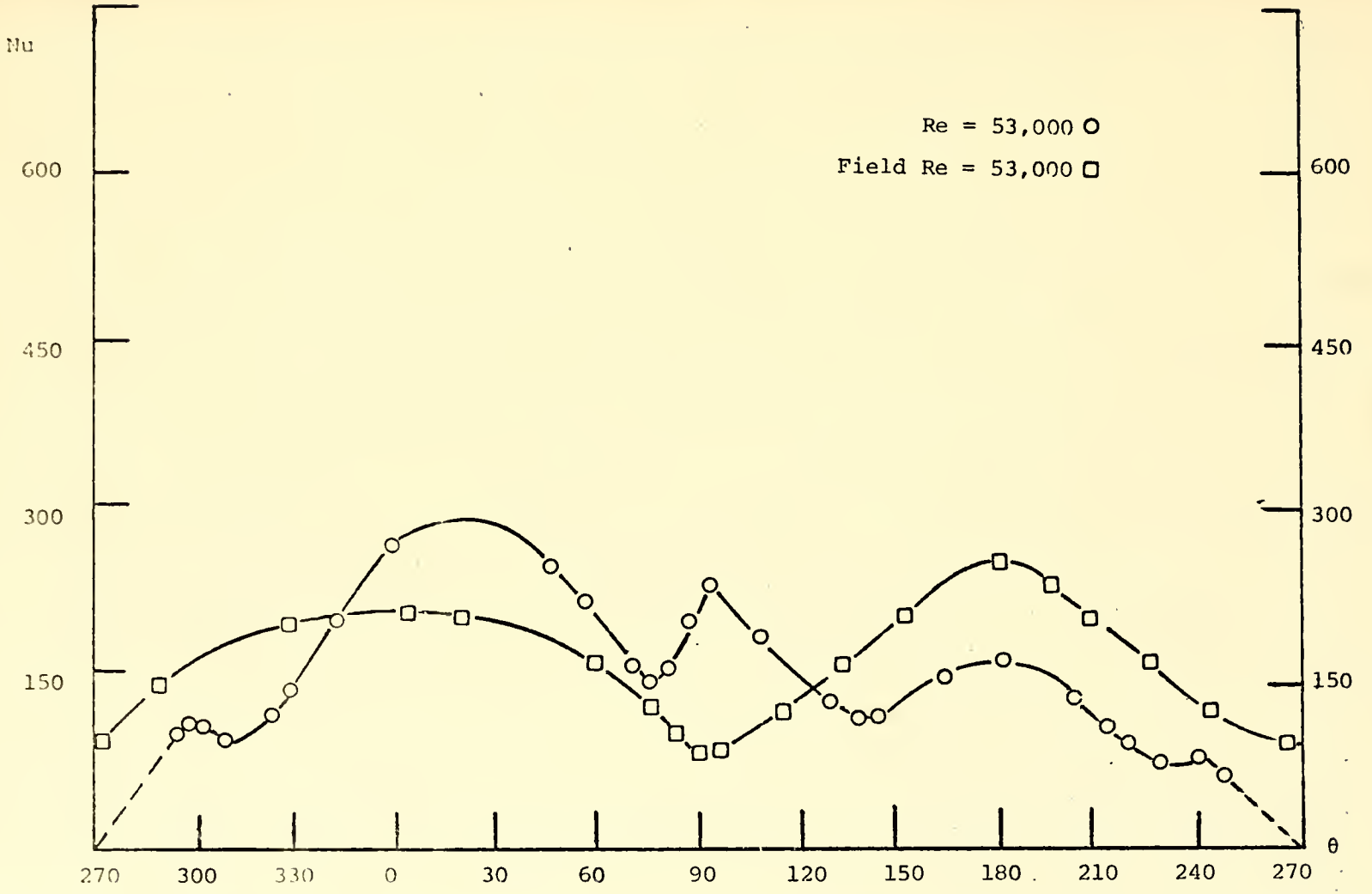

Figure 10. Comparison of heat transfer results with those of Field at a Reynolds number of 53,000.

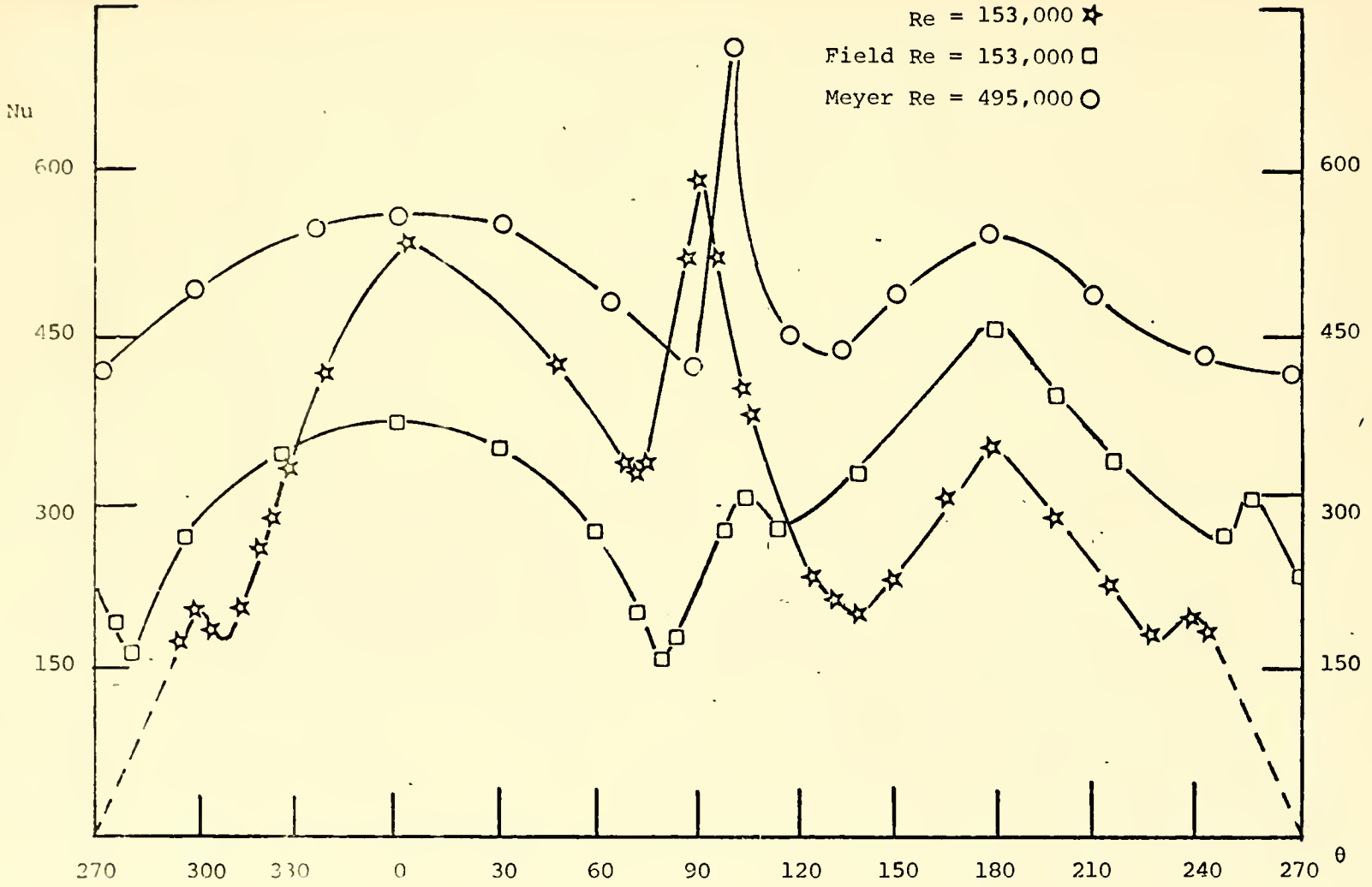

Figure 11. Comparison of heat transfer results obtained at a Reynolds number of 153,000 with those of other investigators.

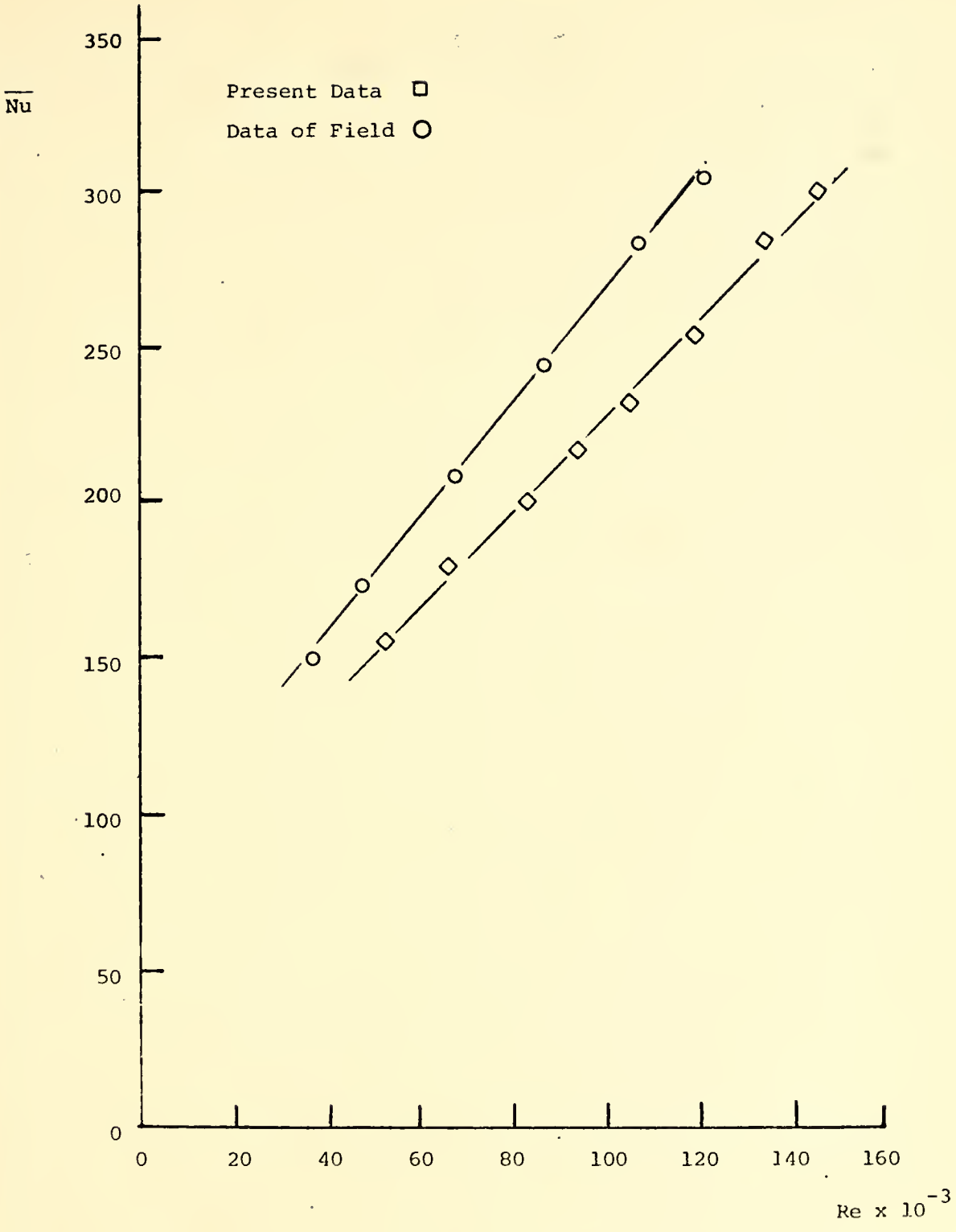

Figure 12. Average Nusselt number versus Reynolds number.

the maximum value to occur at the reattachment point, but this phenomenon was also observed at Reynolds numbers above 300,000.

It is also interesting to note that, despite the lack of correlation between this data and Field's data, the plots of average Nusselt number versus Reynolds number have nearly the same slope in the Reynolds number range between 50,000 and 150,000, with Field's average values being higher than those obtained in this investigation at all Reynolds numbers.

B. PRESSURE EXPERIMENT

Raw data and sample calculations from the two pressure runs are contained in Appendix B. This section contains graphical results of the pressure coefficient versus angular location for Reynolds numbers of 105,000 and 156,000 (Figure 13), and a comparison of the pressure coefficient curve at a Reynolds number of 156,000 with those obtained by Meyer [3] at Reynolds numbers of 153,000 and 495,000 (Figure 14).

The pressure distributions at the two Reynolds numbers tested were in good agreement with the heat transfer results obtained at similar Reynolds numbers. This is especially evident in the higher Reynolds number case. For this case, the pressure coefficient reached a minimum at 73 degrees, and the subsequent upward slope contained a double inflection characteristic of the separation "bubble" region between 75 and 85 degrees. The first inflection point occurred at approximately 78 degrees which corresponds precisely to the laminar separation point found in the heat transfer experiment. Likewise, the second inflection point occurred at approximately 90 degrees which corresponds closely with the 92-degree location of the reattachment point found in the heat transfer experiment. Additionally, the pressure coefficient curve began to flatten at approximately 135

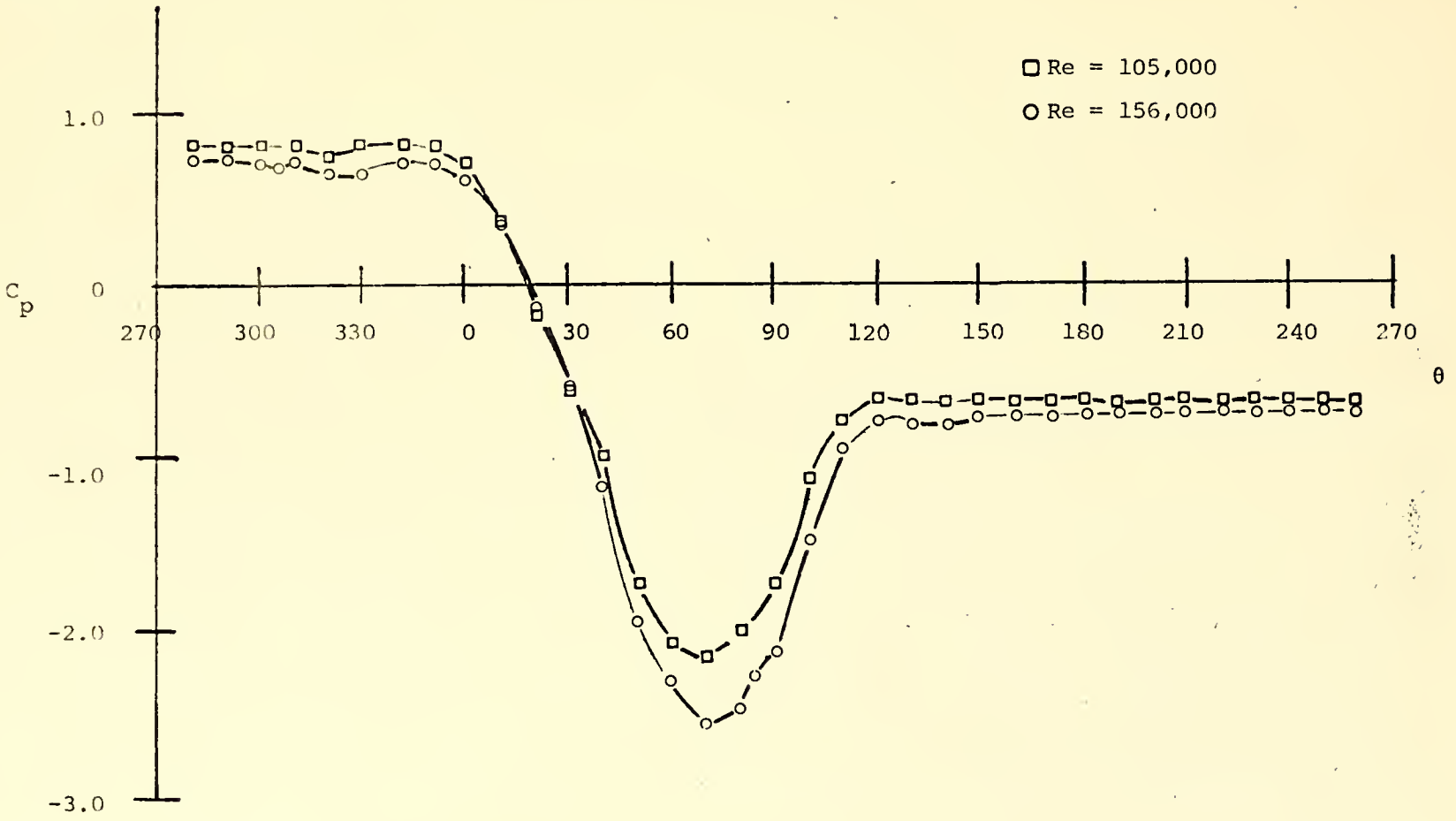

Figure 13. Pressure results at Reynolds numbers of 105,000 and 156,000.

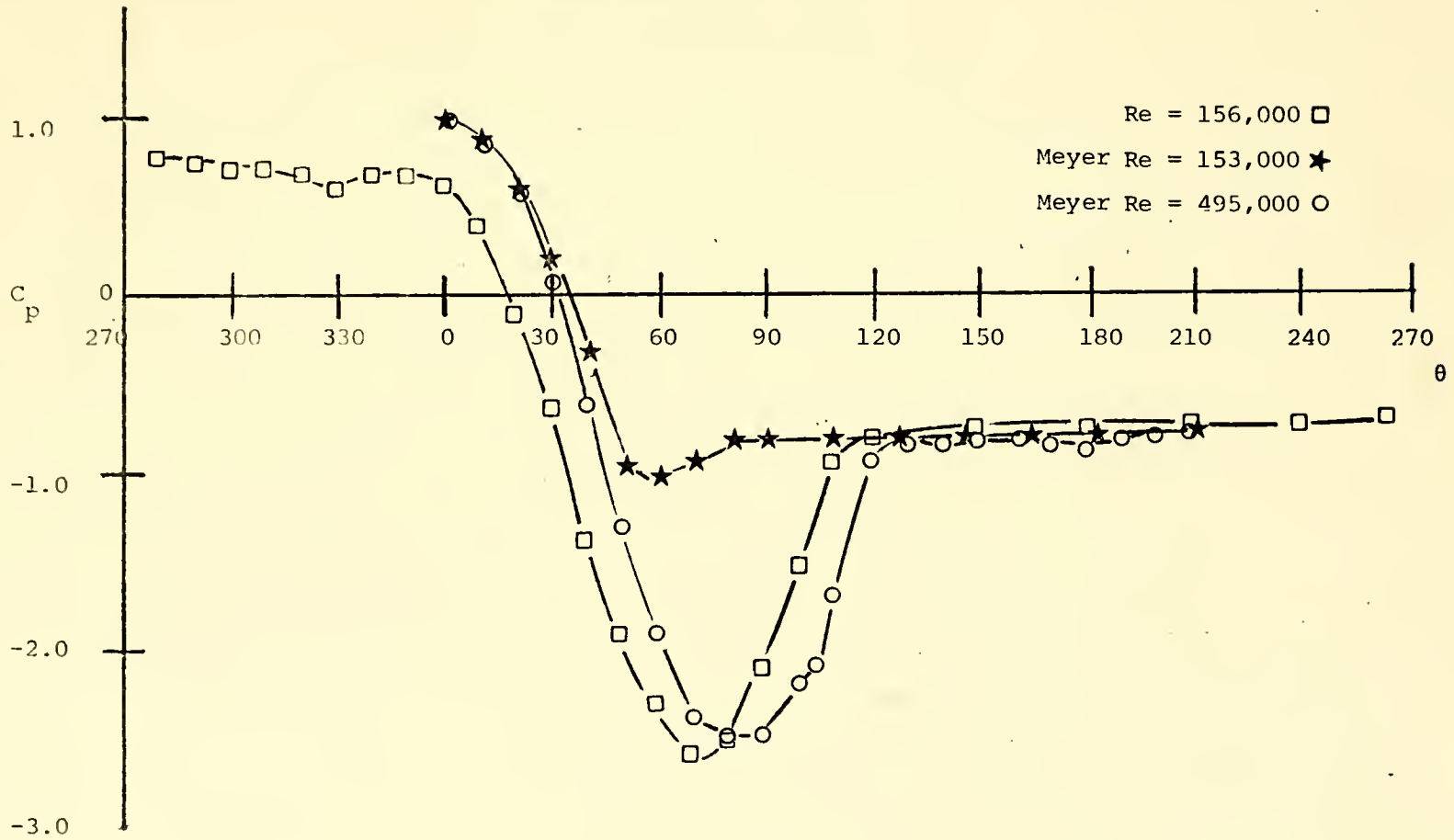

Figure 14. Comparison of Pressure results at a Reynolds number of 156,000 with those of Meyer at Reynolds Numbers of 153,000 and 495,000.

degrees which corresponds favorably with the point of final separation observed at 140 degrees in the heat transfer experiment. Finally, fluctuations in the pressure coefficient curves were noted in the regions corresponding to the locations of the "trapped" vortices which reinforces the heat transfer data in this region.

A comparison of the pressure coefficient curves obtained at a Reynolds number of 156,000 with those of Meyer obtained on one side of a "free" cylinder at Reynolds numbers of 153,000 and 495,000 indicated that the behavior exhibited by the cylinder attached to the flat plate more closely patterned that of a "free" cylinder at much higher Reynolds numbers. In the region between 0 and 180 degrees, the magnitude of the pressure coefficients obtained at a Reynolds number of 156,000 were nearly identical to those of Meyer obtained at a Reynolds number of 495,000, but offset approximately 10 degrees throughout the entire region. This correlates with the fact that the magnitudes of the heat transfer coefficient at this Reynolds number followed closely those of Meyer at Reynolds numbers above 300,000.

C. FLOW VISUALIZATION EXPERIMENT

Because of the limitation in the pump capacity, the highest Reynolds number which could be obtained in this experiment was approximately 10,000. This was well below the Reynolds number range examined in both the heat transfer and pressure experiments, and, as a result, correlation was difficult. However, the behavior observed agreed well with the proposed theory for the subcritical range.

Referring to the regions of the cylinder described in the proposed theory, Region I behaved almost exactly as predicted. The flow was

observed to separate from the flat plate and reattach to the cylinder at a point just aft of the 0 degree mark. Within this separated region, a large turbulent separation vortex was observed, and a series of small, circular, three-dimensional vortices were clearly evident at approximately 30 to 60 degrees from the point of attachment of the cylinder to the plate.

Region II exhibited behavior characteristic of subcritical flow around a "free" cylinder. No separation "bubble" was noted, probably due to the fact that the Reynolds number was too low. However, laminar boundary layer separation was clearly observed at approximately 80 degrees. This behavior was as predicted by the proposed theory for subcritical Reynolds numbers.

Region III was highly turbulent and three-dimensional and was very difficult to interpret with certainty. It did appear, however, that a separated region with its characteristic separation vortex was present. No "trapped" vortices were observed, but the flow appeared to be somewhat stagnant in the region extending approximately 30 degrees forward of the point of attachment of the cylinder to the plate.

VI. CONCLUSIONS AND RECOMMENDATIONS

The theory for the flow around a right circular cylinder attached to a flat plate in a crossflow of air which was proposed in this investigation appears to accurately describe the actual conditions existing at Reynolds numbers based on cylinder diameter from approximately 53,000 to 153,000. The heat transfer data obtained correlates well with the pressure data obtained, and both are in agreement with the proposed theory in a qualitative sense. Quantitatively, both the heat transfer data and the pressure data for Reynolds numbers in the range of 53,000 to 153,000 correlates in the region between 0 and 180 degrees with the data obtained by Meyer [3] for flow around a "free" right circular cylinder in a crossflow of air at Reynolds numbers in the range 300,000 to 500,000.

The flow visualization exhibited consistency with the proposed theory for subcritical flow, but was inconsistent in some regions with the experimental results. This was probably due to the fact that the flow visualization experiment was conducted at a much lower Reynolds number than were the heat transfer and pressure experiments. It is recommended that an attempt be made to refine the existing flow visualization apparatus such that higher Reynolds number flows can be attained. This would give a clearer picture of the flow at Reynolds numbers in the range of 50,000 to 150,000, and correlation with the other data could be made more meaningful.

The liquid crystal technique developed by Field [2] again proved to be an excellent method for quickly and easily obtaining heat transfer data in forced convection environments. Since the problem addressed in this work had not been investigated previously, no measure of comparison is

available for the values of the local Nusselt number obtained. But, the qualitative information displayed by the liquid crystals was verified both by the pressure data and the flow visualization. Continued experiments involving liquid crystals are highly encouraged.

The results obtained in this investigation suggest several areas in which follow-up type investigations might be conducted. First, the present investigation should be extended over a greater Reynolds number range with primary attention being focused on Reynolds numbers below 50,000. This is considered necessary in order to ascertain at what Reynolds number the flow transitions from subcritical to critical for this particular flow configuration. It is felt that such a point does exist because the results of the flow visualization conducted in this investigation suggest subcritical behavior at a Reynolds number of 10,000.

Secondly, an effort should be made to determine at what distance away from the flat plate the cylinder can be moved and not feel the effects of the plate, i.e. at what distance away from the plate will the cylinder behave as a "free" cylinder.

Finally, a study could be undertaken with the same configuration, but with attention being focused on the flat plate rather than the cylinder. This study could be made in the same light as those conducted on forward-facing and rear-facing steps.

APPENDIX A

HEAT TRANSFER DATA AND DATA REDUCTION

The values of the local Nusselt number at various angular locations were determined using the relationship between the convective heat transfer coefficient, h_c, and the surface heat flux produced by Joulean heating, V^2/RA_s. This relationship was developed by Meyer [3] by performing a simple energy balance on an elemental control volume of the Temsheet. The result is

$$h_c = \frac{V^2/RA_s + (kt/r_o^2)d^2T/d\theta^2}{(T-T_\infty)} - h_r$$

where

h_c = convective heat transfer coefficient

V = voltage applied to the test section

R = electrical resistance of the test section

A_s = surface area of the test section

k = thermal conductivity of the test section material

t = thickness of the test section

r_0 = radius of the cylinder

T = temperature at angular location θ

T_∞ = temperature of the air freestream

θ = circumferential location on the cylinder

h_r = radiation heat transfer coefficient = $\sigma F_{1-2}(T+T_\infty)(T^2+T_\infty^2)$

where

σ = Stefan-Boltzman constant = $.1714 \times 10^{-8}$ BTU/hr-ft^2-$^oR^4$

F_{1-2} = radiation exchange factor between cylinder and surroundings

Once h_c has been determined, the Nusselt number can be obtained from the equation

$$Nu = 2h_c r_o / k_{air}$$

The Reynolds number is

$$Re = U_\infty D/\nu$$

where

U_∞ = velocity of the air freestream

D = diameter of the cylinder

ν = kinematic viscosity of air

Field [2] determined that the product kt for Temsheet was on the order of 0.002 BTU/hr - ^oF; hence, it was considered negligibly small for purposes of this investigation.

A sample calculation of the Nusselt number is provided below using the data obtained at a Reynolds number of 153,520 and an angular location of 330 degrees.

$F_{1-2} = 0.9$

$\sigma = .1714 \times 10^{-8}$ BTU/hr-ft^2-$^oR^4$

$T = 111.0^oF = 571^oR$

$T_\infty = 73.1^oF = 533.1^oR$

$U_\infty = 76$ ft/sec

$V = 37.4$ volts

$R = 13.1$ ohms

$D/\nu = 2020$ sec/ft

$2r_o/k_{air} = 22.0$ hr-^oF-ft^2/BTU

$A_s = 0.528$ ft^2

$Re = U_\infty D/\nu = (76 \text{ ft/sec})(2020 \text{ sec/ft}) = 153,520$

$$h = h_c + h_r = \frac{V^2}{RA_s(T-T_\infty)} = \frac{(37.4)^2 \text{ volts}^2}{(13.1)(.528 \text{ ft}^2)(37.9^oF)(.293 \text{ watts/BTU/hr})}$$

$h = 18.2$ BTU/hr-ft^2-^oF

$h_r = (.9)(.1714 \times 10^{-8}$ BTU/hr-ft^2-$^oR^4)(571+533.1)(571^2+533.1^2)$ $^oR^3$

$h_r = 1.04$ BTU/hr-ft^2-^oF

$h_c = 17.17$ BTU/hr-ft^2-^oF

Nu = (17.17BTU/hr-ft^2-^oF)(22.0 hr-ft^2-^oF/BTU)

Nu = 377.7

The data sheets for all nine heat transfer runs follow.

DATA

Ave. Air Temp.=69.7°F; D/ℓ=2044 sec/ft — Date: 10 SEPT 74

Air Speed=.36 cm.H_2O — Time: 1930

=25.1 ft/sec — Resistance= 13.3 Ω

Re= 51,304

Film Temp.=90.4°F; D/k=22.1 hr-°F-ft^2/BTU

θ	CRY TEMP	AIR TEMP	V	h	h_r	h_c	Nu	Comments
78	111.0	69.5	25.6	7.67	1.03	6.64	146.74	→ SEPARATION
124	111.0	69.5	25.6	7.67	1.03	6.64	146.74	
163	111.0	69.5	25.6	7.67	1.03	6.64	146.74	
200	111.0	69.5	25.6	7.67	1.03	6.64	146.74	
327	111.0	69.5	25.6	7.67	1.03	6.64	146.74	
303	112.3	69.5	25.6	7.44	1.03	6.41	141.66	
71	111.0	69.6	28.0	9.20	1.03	8.17	180.56	
82	111.0	69.6	28.0	9.20	1.03	8.17	180.56	
111	111.0	69.6	28.0	9.20	1.03	8.17	180.56	
181	112.3	69.6	28.0	8.92	1.03	7.89	174.37	
332	111.0	69.6	28.0	9.20	1.03	8.17	180.56	
92	111.0	69.6	31.9	11.95	1.03	10.92	241.33	→ REATTACHMENT
56	111.0	69.6	31.9	11.95	1.03	10.92	241.33	
344	111.0	69.6	31.9	11.95	1.03	10.92	241.33	
44	111.0	69.6	32.8	12.63	1.03	11.60	256.36	
353	111.0	69.6	32.8	12.63	1.03	11.60	256.36	
4	111.0	69.6	35.3	14.63	1.03	13.60	278.47	
128	111.0	69.8	24.4	7.02	1.03	5.99	132.38	
154	111.0	69.8	24.4	7.02	1.03	5.99	132.38	
204	111.0	69.8	24.4	7.02	1.03	5.99	132.38	
33	1		2	7.0	1			
140	109.8	69.8	23.2	6.54	1.03	5.51	121.77	
240	111.0	69.8	23.2	6.35	1.03	5.32	117.57	
303	111.0	69.8	23.2	6.35	1.03	5.32	117.57	
216	111.0	69.8	21.9	5.66	1.03	4.63	102.32	
315	109.8	69.8	21.9	5.83	1.03	4.80	106.08	
298	111.0	69.8	21.9	5.66	1.03	4.63	102.32	
224			21.9	5.66				
240	111.0	69.8	23.2	6.35	1.03	5.32	117.57	
295	111.0	69.8	23.2	6.35	1.03	5.32	117.57	

DATA

Ave. Air Temp.=70.1 °F; D/$\mathcal{L}$=2011 $\frac{\text{sec}}{\text{ft}}$

Air Speed=.60 cm.H_2O

= 32 ft/sec

Re= 65,312

Film Temp.=90.6 °F; D/k=22.1 hr-°F-ft^2/BTU

Date: 10 SEPT 74

Time: 2015

Resistance=13.3 Ω

θ	CRT TEMP	AIR TEMP	V	h	h_r	h_c	Nu	Comments
75	117.8	70.1	27.6	9.25	1.03	8.22	183.43	
123	111.0	70.1	27.6	9.05	1.03	8.02	177.24	
163	111.0	70.1	27.6	9.05	1.03	8.02	177.24	
201	111.0	70.1	27.6	9.05	1.03	8.02	177.24	
326	111.0	70.1	27.6	9.05	1.03	8.02	177.24	
70	111.0	70.1	29.1	10.06	1.03	9.03	199.56	
80	111.0	70.1	29.1	10.06	1.03	9.03	199.56	
118	111.0	70.1	29.1	10.06	1.03	9.03	199.56	
180	111.0	70.1	29.1	10.06	1.03	9.03	199.56	
328	111.0	70.1	29.1	10.06	1.03	9.03	199.56	
91	114.5	70.1	34.8	14.94	1.03	13.36	295.26	RECIRCULATING
45	114.5	70.1	34.8	14.94	1.03	13.36	295.26	
352	114.5	70.1	34.8	14.94	1.03	13.36	295.26	
3	111.0	70.1	37.3	16.58	1.03	15.55	342.55	
84	111.0	70.1	31.5	11.79	1.03	10.76	237.80	
103	111.0	70.1	31.5	11.79	1.03	10.76	237.80	
58	111.0	70.1	31.5	11.79	1.03	10.76	237.80	
337	111.0	70.1	31.5	11.79	1.03	10.76	237.80	
131	111.0	70.1	25.0	7.45	1.03	6.40	141.44	
182								
303			25.0	7.45	1.03	6.40	141.44	
21								
302	112.3		23.5	.36			117.71	
297			22.0	5.75	1.03	4.72	104.31	
305			22.0	5.75	1.03	4.72	104.31	
					1.03	4.72		
	112.3							
244	111.0		20.9	5.11		4.12	91.4	
230			21.4					

DATA

Ave. Air Temp.=70.3°F; D/f=20.0 sec/ft — Date: 10 SEPT 74

Air Speed=.98 cm.H_2O — Time: 2055

= 41 ft/sec — Resistance=13.2 Ω

Re= 83,640

Film Temp.=90.7°F; D/k=22.1 hr-°F-ft^2/BTU

θ	CRY TEMP	AIR TEMP	V	h	h_r	h_c	Nu	Comments
75	111.0	70.3	28.6	9.98	1.03	8.95	197.80	- SEPARATION
123	111.0	70.3	28.6	9.98	1.03	8.95	197.80	
201	111.0	70.3	28.6	9.98	1.03	8.95	197.80	
166	111.0	70.3	28.6	9.98	1.03	8.95	197.80	
327	111.0	70.3	28.6	9.98	1.03	8.95	197.80	
69	111.0	70.3	30.5	11.19	1.03	10.16	224.54	
81	111.0	70.3	30.5	11.19	1.03	10.16	224.54	
114	111.0	70.3	30.5	11.19	1.03	10.16	224.54	
120	111.0	70.3	30.5	11.19	1.03	10.16	224.54	
328	111.0	70.3	30.5	11.19	1.03	10.16	224.54	
59	111.0	70.3	33.0	13.10	1.03	12.07	266.75	
93	111.0	70.3	33.0	13.10	1.03	12.07	266.75	
105	111.0	70.3	33.0	13.10	1.03	12.07	266.75	
334	111.0	70.3	33.0	13.10	1.03	12.07	266.75	
45	111.0	70.3	35.5	15.16	1.03	14.13	310.27	
86	111.0	70.3	35.5	15.16	1.03	14.13	310.27	
102	111.0	70.3	35.5	15.16	1.03	14.13	310.27	
344	111.0	70.3	35.5	15.16	1.03	14.13	310.27	
2	[illegible]	70.3	37.4	[illegible]	[illegible]	[illegible]	[illegible]	
[illegible]	[illegible]	[illegible]	[illegible]	[illegible]	[illegible]	16.20	[illegible]	
			[illegible]	[illegible]		7.[illegible]	[illegible]	
153	111.[illegible]	70.3	24.5	8.45	1.03	7.42	163.[illegible]	
[illegible]		70.3	[illegible]	[illegible]	[illegible]	[illegible]	[illegible]	
2[illegible]	111.0	70.2	24.6	7.26	1.03	6.23	[illegible]	
321	111.0	70.2	24.6	7.26	1.03	6.23	137.68	
221	111.0	70.2	23.[illegible]	[illegible]	1.03	5.[illegible]	125.[illegible]	
240	111.0	70.2	23.[illegible]	[illegible]	1.03	5.[illegible]	125.74	
	[illegible]				[illegible]			
[illegible]	[illegible]	[illegible]	[illegible]	[illegible]	[illegible]	[illegible]	[illegible]	
[illegible]	[illegible]	70.2	22.4	[illegible]	1.03	[illegible]	[illegible]	
	[illegible]		[illegible]	[illegible]		4.11	[illegible]	
[illegible]	[illegible]	[illegible]	[illegible]	[illegible]	[illegible]	[illegible]	[illegible]	

DATA

Ave. Air Temp.= 68.6°F; D/r = 200 sec/ft

Air Speed= 1.21 cm.H_2O

= 45.6 ft/sec

Re= 93,526

Film Temp.= 88°F; D/k= 22.1 hr-°F-ft^2/BTU

Date: 12 SEPT 74

Time: 1130

Resistance= 13.4 Ω

θ	CRT TEMP	AIR TEMP	V	h	h_r	h_c	Nu	Comments
75	111.0	68.1	31.0	10.81	1.03	9.78	214.14	
123	↓	↓	↓	↓	↓	↓	↓	
162	↓	↓	↓	↓	↓	↓	↓	
202	↓	↓	↓	↓	↓	↓	↓	
326	↓	↓	↓	↓	↓	↓	↓	
68	111.0	68.2	33.6	12.72	1.03	11.69	258.25	
80	↓	↓	↓	↓	↓	↓	↓	
112	↓	↓	↓	↓	↓	↓	↓	
180	↓	↓	↓	↓	↓	↓	↓	
331	↓	↓	↓	↓	↓	↓	↓	
52	111.0	68.3	36.4	14.97	1.03	13.94	308.07	
84	↓	↓	↓	↓	↓	↓	↓	
102	↓	↓	↓	↓	↓	↓	↓	
334	↓	↓	↓	↓	↓	↓	↓	
36	111.0	68.5	38.3	16.95	1.03	15.92	345.20	
86	↓	↓	↓	↓	↓	↓	↓	
98	↓	↓	↓	↓	↓	↓	↓	
353	↓	↓	↓	↓	↓	↓	↓	
8	↓	68.7	40.2	18.93	↓	17.90	381.58	
92	↓	↓	↓	↓	↓	↓	↓	
1	↓	↓	27.6	↓	↓	↓	↓	
150	↓	↓	↓	↓	↓	↓	↓	
2	↓	↓	↓	↓	↓	↓	↓	
↓	↓	↓	↓	↓	↓	↓	↓	
217	111.0	69.0	25.4	7.41	1.03	6.38	136.00	
320	↓	↓	↓	↓	↓	↓	↓	
284	112.3	↓	25.4	7.41	1.03	6.38	136.14	
2	↓	↓	↓	↓	↓	↓	↓	
3	"	↓	↓	6	↓	↓	137	
234	↓	↓	↓	↓	↓	↓	↓	
311	↓	↓	↓	↓	↓	↓	↓	
3	↓	↓	↓	↓	↓	↓	↓	
247	111.0	69.2	33.5	6.31	1.03	5.28	112.71	
295	↓	↓	↓	↓	↓	↓	↓	
308	↓	↓	↓	↓	↓	↓	↓	

DATA

Ave. Air Temp.=69.8 °F; D/k=.044 $\frac{sec}{ft}$ Date: 12 SEPT 74

Air Speed=1.50 cm.H_2O Time: 1205

= 51 ft/sec Resistance=13.4 Ω

Re= 104,244

Film Temp.=90.4 °F; D/k= 22.1 hr-°F-ft^2/BTU

θ	CRT TEMP	AIR TEMP	V	h	h_r	h_c	Nu	Comments
75	[illegible]	69.4	31.2	11.05	[illegible]	10.32	221.44	-SEPARATION
125	↓	↓	↓	↓	↓	↓	↓	
158	↓	↓	↓	↓	↓	↓	↓	
204	↓	↓	↓	↓	↓	↓	↓	
326	↓	↓	↓	↓	↓	↓	↓	
63	111.0	69.7	34.2	13.66	1.03	12.63	279.12	
81	↓	↓	↓	↓	↓	↓	↓	
110	↓	↓	↓	↓	↓	↓	↓	
182	↓	↓	↓	↓	↓	↓	↓	
332	↓	↓	↓	↓	↓	↓	↓	
48	111.0	69.7	37.4	16.36	1.03	15.31	338.88	
81	↓	↓	↓	↓	↓	↓	↓	
102	↓	↓	↓	↓	↓	↓	↓	
336	↓	↓	↓	↓	↓	↓	↓	
32	111.0	69.9	39.0	17.85	1.03	16.82	371.72	
85	↓	↓	↓	↓	↓	↓	↓	
98	↓	↓	↓	↓	↓	↓	↓	
348	↓	↓	↓	↓	↓	↓	↓	
8	[illegible]	[illegible]	41.4	[illegible]	[illegible]	[illegible]	421.82	
92	[illegible]	[illegible]	[illegible]	[illegible]	[illegible]	[illegible]	[illegible]	
10	[illegible]	[illegible]	[illegible]	[illegible]	[illegible]	[illegible]	[illegible]	
152	↓	↓	↓	↓	↓	↓	↓	
212	↓	↓	↓	↓	↓	↓	↓	
[illegible]	↓	↓	↓	↓	↓	↓	↓	
218	[illegible]	70.2	28.2	8.12	1.03	7.09	[illegible]	
240	113.3	70.2	26.2	7.87	1.03	6.84	151.16	
219	111.0	70.2	28.2	8.12	1.03	7.09	156.68	
302	113.3	70.2	26.2	7.87	1.03	6.84	151.16	
[illegible]	[illegible]	[illegible]	[illegible]	[illegible]	[illegible]	[illegible]	[illegible]	
257	↓	↓	↓	↓	↓	↓	↓	
243	↓	↓	↓	↓	↓	↓	↓	
[illegible]	↓	↓	↓	↓	↓	↓	↓	
30.1	↓	↓	↓	↓	↓	↓	↓	
316	↓	↓	↓	↓	↓	↓	↓	

DATA

Ave. Air Temp.= 70.8 °F; $D/\nu = 2039 \frac{sec}{ft}$

Air Speed= 1.92 cm.H_2O

= 58 ft/sec

Re= 118,262

Film Temp.= 90.9 °F; D/k= 22.1 hr-°F-ft^2/BTU

Date: 12 SEPT 74

Time: 1248

Resistance= 13.4 Ω

θ	CRT TEMP	AIR TEMP	V	h	h_r	h_c	Nu	Comments
76	111.0	70.6	31.8	12.67	1.[illegible]	11.64	245.98	-SEPARATION
121	↓	↓	↓	↓	↓	↓	↓	
163	↓	↓	↓	↓	↓	↓	↓	
205	↓	↓	↓	↓	↓	↓	↓	
326	↓	↓	↓	↓	↓	↓	↓	
81	111.0	70.7	34.8	14.30	1.03	13.47	297.69	
67	↓	↓	↓	↓	↓	↓	↓	
182	↓	↓	↓	↓	↓	↓	↓	
229	↓	↓	↓	↓	↓	↓	↓	
50	111.0	70.8	37.6	16.[illegible]	1.03	15.93	352.05	
83	↓	↓	↓	↓	↓	↓	↓	
104	↓	↓	↓	↓	↓	↓	↓	
336	↓	↓	↓	↓	↓	↓	↓	
6	111.0	71.0	42.5	21.78	1.78	20.05	459.56	
356	112.3	71.0	42.5	21.10	[illegible]	21.07	443.50	
88	111.0	71.0	42.5	21.78	1.03	20.75	459.18	
90	↓	↓	↓	↓	↓	↓	↓	
91	111.0	71.0	44.9	24.31	1.03	23.28	510.[illegible]	-REATTACHMENT
125	111.0	71.0	25.2	[illegible]	1.05	9.[illegible]	19[illegible]	
[illegible]	↓	↓	↓	[illegible]	↓	↓	↓	
[illegible]	↓	↓	↓	[illegible]	↓	↓	↓	
220	111.0	71.0	26.2	8.[illegible]	1.03	7.27	1[illegible]41	
[illegible]	↓	↓	↓	[illegible]	↓	↓	↓	
[illegible]	↓	↓	↓	[illegible]	↓	↓	↓	
29[illegible]	↓	↓	↓	[illegible]	↓	↓	↓	
302	↓	↓	↓	[illegible]	↓	↓	↓	
31[illegible]	↓	↓	↓	[illegible]	↓	↓	↓	
33[illegible]	10[illegible]8	71.0	24.9	7.78	1.03	6.70	14[illegible]	
[illegible]	↓	↓	↓	[illegible]	↓	↓	[illegible]	
29.1	↓	↓	↓	[illegible]	↓	↓	↓	
30[illegible]	10[illegible]	71.0	24.9	7.78	↓	↓	↓	
[illegible]	↓	↓	↓	[illegible]	↓	↓	↓	
[illegible]	↓	↓	↓	[illegible]	↓	↓	↓	

DATA

Ave. Air Temp.=703 °F; $D/k = 2040 \frac{sec}{ft}$ Date: 13 SEPT 74

Air Speed=2.40 cm.H_2O Time: 1130

= 65 ft/sec Resistance= 13.1 Ω

Re= 132,600

Film Temp.=90.6 °F; D/k=22.1 hr-°F-ft^2/BTU

θ	CRY TEMP	AIR TEMP	V	h	h_r	h_c	Nu	Comments
76	111.0	69.5	32.5	13.34	1.03	12.31	222.05	-SEPARATION
121								
160								
204								
326								
69	111.2	69.8	36.5	15.94	1.03	14.93	329.95	
81								
108								
182								
330								
51	111.2	69.9	39.7	18.92	1.03	17.89	395.57	
50								
100								
337								
26	111.0	70.1	42.1	21.32	1.03	20.35	449.74	
86								
99								
345								
11	111.2	70.3	44.6	24.2	1.03	23.24	513.29	
16								
-								
41	111.0	70.4	46.9	26.73	1.03	25.70	567.97	-REATTACHMENT
120		70.7		11.2				
211								
322								
219	111.0	70.8	28.5	9.52	1.03	8.49	194.08	
278								
21								
32	112.3	70.8	32	0	1.03	8.11	172	
317	111.1	70.9	28.5	9.52	1.03	8.49	194.48	
-		71	28		1			
241								
296								
303								
313								

DATA

Ave. Air Temp.=71.8°F; D/ℓ =2031 $\frac{sec}{ft}$ Date: 13 SEPT 74

Air Speed=2.80cm.H_2O Time: 1205

= 70 ft/sec Resistance= 13.1 Ω

Re= 142,170

Film Temp.=91.4°F; D/k= 22.4 hr-°F-ft^2/BTU

θ	CRT TEMP	AIR TEMP	V	h	h_r	h_c	Nu	Comments
77	111.0	71.4	34.0	14.90	1.03	13.87	293.42	- SEPARATION
119	↓	↓	↓	↓	↓	↓	↓	
158	↓	↓	↓	↓	↓	↓	↓	
202	↓	↓	↓	↓	↓	↓	↓	
324	↓	↓	↓	↓	↓	↓	↓	
71	111.0	71.5	36.9	17.01	1.03	15.98	353.16	
83	↓	↓	↓	↓	↓	↓	↓	
108	↓	↓	↓	↓	↓	↓	↓	
182	↓	↓	↓	↓	↓	↓	↓	
330	↓	↓	↓	↓	↓	↓	↓	
49	111.0	71.6	40.1	20.14	1.04	19.10	422.11	
85	↓	↓	↓	↓	↓	↓	↓	
102	↓	↓	↓	↓	↓	↓	↓	
338	↓	↓	↓	↓	↓	↓	↓	
2	111.0	71.9	45.0	25.56	1.04	24.52	541.89	
88	↓	↓	↓	↓	↓	↓	↓	
95	↓	↓	↓	↓	↓	↓	↓	
91	111.0	71.9	47.5	28.47	1.04	27.43	606.20	- REATTACHMENT
127	111.0	72.0	49.9	31.1	1.04	30.07	664.97	
149	↓	↓	↓	↓	↓	↓	↓	
216	↓	↓	↓	↓	↓	↓	↓	
321	↓	↓	↓	↓	↓	↓	↓	
224	111.0	72.1	2.5	↓	↓	↓	↓	
240	↓	↓	↓	↓	↓	↓	↓	
249	↓	↓	↓	↓	↓	↓	↓	
303	↓	↓	↓	↓	↓	↓	↓	
312	↓	↓	↓	↓	↓	↓	↓	
231	↓	↓	↓	↓	↓	↓	↓	
241	↓	↓	↓	↓	↓	↓	↓	
270	↓	↓	↓	↓	↓	↓	↓	
[illegible]	↓	↓	↓	↓	↓	↓	↓	
294	↓	72.2	44.0	8.0	↓	↓	↓	
292	↓	↓	↓	↓	↓	↓	↓	

DATA

Ave. Air Temp.=735°F; D/k=2000 sec/ft — Date: 10 SEPT 1974

Air Speed=3.58 cm.H_2O — Time: 1235

= 76 ft/sec — Resistance=13.1 Ω

Re= 153,520

Film Temp.=92.3°F; D/k=22.0 hr-°F-ft^2/BTU

θ	CRT TEMP	AIR TEMP	V	h	h_r	h_c	Nu	Comments
78	111.2	73.1	5[illegible]	[illegible]	1.04	[illegible]	3[illegible]	- SEPARATION
119	↓	↓	↓	↓	↓	↓	↓	
167	↓	↓	↓	↓	↓	↓	↓	
200	↓	↓	↓	↓	↓	↓	↓	
356	↓	↓	↓	↓	↓	↓	↓	
71	111.0	73.1	37.4	18.21	1.04	17.17	377.74	
82	↓	↓	↓	↓	↓	↓	↓	
108	↓	↓	↓	↓	↓	↓	↓	
182	↓	↓	↓	↓	↓	↓	↓	
330	↓	↓	↓	↓	↓	↓	↓	
51	111.0	73.2	40.4	21.31	1.04	20.27	445.94	
85	↓	↓	↓	↓	↓	↓	↓	
104	↓	↓	↓	↓	↓	↓	↓	
337	↓	↓	↓	↓	↓	↓	↓	
0	111.0	73.2	45.3	26.93	1.04	25.89	569.58	
88	↓	↓	↓	↓	↓	↓	↓	
98	↓	↓	↓	↓	↓	↓	↓	
92	111.1	73.4	42.2	31.27	1.04	30.23	476.06	- REATTACHMENT
123	111.2	73.5	21	12.[illegible]	1.04	11.[illegible]	257.8	
151	↓	↓	↓	↓	↓	↓	↓	
[illegible]	↓	↓	↓	↓	↓	↓	↓	
323	↓	↓	↓	↓	↓	↓	↓	
218	1[illegible]	[illegible]	[illegible]	[illegible]	[illegible]	[illegible]	[illegible]	
[illegible]	↓	↓	↓	↓	↓	↓	↓	
299	111.0	73.7	29.[illegible]	11.34	[illegible]	10.[illegible]	227.04	
316	↓	↓	↓	↓	↓	↓	↓	
221	111.0	7[illegible]	28.2	10.58	1.04	9.54	207.88	
241	↓	↓	↓	↓	↓	↓	↓	
[illegible]	↓	↓	↓	↓	↓	↓	↓	
3[illegible]	↓	↓	↓	↓	↓	↓	↓	
245	111.0	[illegible]	24.4	[illegible]	[illegible]	8.11	19[illegible]	

APPENDIX B

PRESSURE DATA AND DATA REDUCTION

The values of the pressure coefficient were determined from the formula

$$C_p = \frac{P_\theta - P_s}{\frac{1}{2} \rho U_\infty^2}$$

where

C_p = pressure coefficient

P_θ = static pressure on the cylinder surface at angular location θ

P_s = static pressure in the wind tunnel test section

ρ = density of air

U_∞ = air free stream velocity

Meyer [3] had determined previously that the quantity $\frac{1}{2} \rho U_\infty^2$ could be represented by the difference in static pressure between the wind tunnel plenum chamber and the wind tunnel test section. Therefore,

$$\frac{1}{2} \rho U_\infty^2 = P_{pc} - P_s$$

where

P_{pc} = static pressure in the wind tunnel plenum chamber

A sample calculation of the pressure coefficient is provided below using data obtained at a Reynolds number of 156,180 and an angular location of 90 degrees

P_θ = 12.05 in. H_2O

P_{pc} = 4.02 in. H_2O

P_s = 6.58 in. H_2O

$$C_p = (13.05 - 6.58)/(4.02 - 6.58)$$

$$C_p = -2.14$$

The data for the two pressure runs follow.

PRESSURE DATA

Air Speed= 1.50 cm.H_2O

= 51 ft/sec

Air Temp.= 66.5 °F

D/ν= 2065 sec/ft

Date: 21 OCTOBER 74

Time: 0915

Re= 105,315

θ	P_s	P_{pc}	P_θ	C_p
0	7.20	[illegible]	6.45	[illegible]
5	[illegible]	[illegible]	[illegible]	.555
10	7.19	[illegible]	[illegible]	[illegible]
15	7.20	[illegible]	6.99	.189
20	7.20	[illegible]	[illegible]	[illegible]
[illegible]	[illegible]	[illegible]	[illegible]	[illegible]
[illegible]	[illegible]	[illegible]	7.55	[illegible]
[illegible]	7.10	[illegible]	[illegible]	[illegible]
40	[illegible]	6.08	[illegible]	[illegible]
45	[illegible]	[illegible]	[illegible]	[illegible]
50	[illegible]	[illegible]	9.13	-1.75
55	[illegible]	[illegible]	[illegible]	-1.97
60	[illegible]	[illegible]	9.31	[illegible]
65	[illegible]	[illegible]	[illegible]	[illegible]
[illegible]	7.10	[illegible]	[illegible]	[illegible]
[illegible]	[illegible]	[illegible]	[illegible]	[illegible]
[illegible]	[illegible]	[illegible]	[illegible]	[illegible]
[illegible]	7.19	[illegible]	[illegible]	[illegible]
[illegible]	[illegible]	[illegible]	9.13	[illegible]
[illegible]	7.20	[illegible]	8.99	[illegible]
[illegible]	7.10	[illegible]	[illegible]	[illegible]
105	[illegible]	[illegible]	[illegible]	[illegible]
[illegible]	[illegible]	[illegible]	[illegible]	[illegible]
[illegible]	[illegible]	[illegible]	[illegible]	[illegible]
[illegible]	[illegible]	[illegible]	[illegible]	-.712
[illegible]	[illegible]	[illegible]	[illegible]	[illegible]
[illegible]	[illegible]	[illegible]	[illegible]	[illegible]
[illegible]		[illegible]	[illegible]	[illegible]

θ	P_s	P_{pc}	P_θ	C_p
[illegible]	7.20	[illegible]	[illegible]	[illegible]
[illegible]	7.20	[illegible]	[illegible]	[illegible]
[illegible]	7.19	[illegible]	[illegible]	[illegible]
[illegible]	7.20	[illegible]	[illegible]	[illegible]
[illegible]	7.20	[illegible]		[illegible]
[illegible]	7.20	[illegible]	[illegible]	[illegible]
[illegible]	[illegible]	[illegible]	7.95	[illegible]
[illegible]	7.19	[illegible]	[illegible]	[illegible]
[illegible]	[illegible]	6.08	[illegible]	[illegible]
[illegible]	[illegible]	6.08	7.93	-.667
[illegible]	[illegible]	[illegible]	7.95	[illegible]
[illegible]	[illegible]	[illegible]	7.91	[illegible]
[illegible]	[illegible]	[illegible]	[illegible]	[illegible]
[illegible]	[illegible]	[illegible]	[illegible]	[illegible]
[illegible]	[illegible]	[illegible]	[illegible]	[illegible]
[illegible]	[illegible]	[illegible]	[illegible]	[illegible]
260	[illegible]	[illegible]	[illegible]	[illegible]
265	7.19	[illegible]	[illegible]	[illegible]
[illegible]	7.20	[illegible]	[illegible]	[illegible]
[illegible]	[illegible]	[illegible]	[illegible]	[illegible]
[illegible]	[illegible]	6.09	[illegible]	[illegible]
[illegible]	7.20	[illegible]	[illegible]	[illegible]
[illegible]	[illegible]		[illegible]	[illegible]
[illegible]	[illegible]		[illegible]	[illegible]
	[illegible]			
[illegible]	[illegible]			
[illegible]	[illegible]	[illegible]	[illegible]	[illegible]
[illegible]	[illegible]		[illegible]	[illegible]
[illegible]	[illegible]		[illegible]	[illegible]
[illegible]				

PRESSURE DATA

Air Speed= 3.58 cm.H_2O

= 76 ft/sec

Air Temp.= 68 °F

D/ν= 2055 sec/ft

Date: 22 OCTOBER 74

Time: 1505

Re= 156,180

θ	P_s	P_{pc}	$P_θ$	C_p
0	[illegible]	4.32	[illegible]	[illegible]
5			5.25	[illegible]
10			[illegible]	[illegible]
15			6.13	.176
[illegible]			6.85	-.105
25			[illegible]	[illegible]
[illegible]			8.20	[illegible]
[illegible]			9.15	-1.00
[illegible]			9.89	-1.29
45			[illegible]	[illegible]
50			[illegible]	[illegible]
55			[illegible]	[illegible]
60			[illegible]	[illegible]
65			[illegible]	[illegible]
70			[illegible]	[illegible]
[illegible]			[illegible]	[illegible]
[illegible]			[illegible]	[illegible]
85			[illegible]	[illegible]
90			[illegible]	-2.14
[illegible]			11.45	[illegible]
100			10.42	[illegible]
[illegible]			[illegible]	[illegible]
			[illegible]	
[illegible]			[illegible]	[illegible]
[illegible]				[illegible]
[illegible]			[illegible]	[illegible]
[illegible]			[illegible]	[illegible]
[illegible]			[illegible]	[illegible]
[illegible]			[illegible]	[illegible]
[illegible]				

θ	P_s	P_{pc}	$P_θ$	C_p
[illegible]	6.55	4.02	[illegible]	[illegible]
[illegible]			[illegible]	[illegible]
[illegible]			[illegible]	-.742
[illegible]			[illegible]	[illegible]
[illegible]			[illegible]	-.742
[illegible]			[illegible]	[illegible]
210			[illegible]	[illegible]
215			[illegible]	[illegible]
220			[illegible]	-.723
[illegible]			[illegible]	-.730
[illegible]			[illegible]	[illegible]
[illegible]			[illegible]	[illegible]
[illegible]			[illegible]	[illegible]
245			[illegible]	[illegible]
250			[illegible]	[illegible]
[illegible]			[illegible]	[illegible]
[illegible]			[illegible]	[illegible]
[illegible]			[illegible]	[illegible]
270			8.10	-.594
275			[illegible]	[illegible]
280			11.65	[illegible]
[illegible]			[illegible]	[illegible]
			[illegible]	[illegible]
[illegible]			[illegible]	[illegible]
[illegible]			[illegible]	[illegible]
[illegible]			[illegible]	[illegible]
[illegible]			[illegible]	[illegible]
			[illegible]	
[illegible]			[illegible]	
[illegible]				

APPENDIX C

UNCERTAINTY ANALYSIS

Uncertainty calculations were performed to ascertain the degree of uncertainty in the final results. The method of Kline and McClintock described in reference 19 was used.

Uncertainties existed in the following measured variables: voltage, resistance, cylinder geometry, surface temperature, Temsheet emissivity, angular location, manometer pressure drop, all pressures in the pressure experiment, and properties of air. The uncertainties associated with the latter were considered negligible.

TOTAL HEAT TRANSFER COEFFICIENT, h

The total heat transfer coefficient was calculated from the equation

$$h = \frac{V^2/R}{A_s(T-T_\infty)}$$

Therefore, the uncertainty in the heat transfer coefficient is expressed as

$$\frac{\omega_h}{h} = \sqrt{\left(\frac{2\omega_V}{V}\right)^2 + \left(\frac{\omega_R}{R}\right)^2 + \left(\frac{\omega_{A_S}}{A_S}\right)^2 + \left(\frac{\omega_{\Delta T}}{\Delta T}\right)^2}$$

For the experimental run at a Reynolds number of 153,520 and an angular location of 330 degrees,

$V = 37.4 \pm 0.1$ volts (20 to 1)

$R = 13.1 \pm 0.2$ ohms (20 to 1)

$\Delta T = 37.9 \pm 0.5\ ^{o}F$ (20 to 1)

$A_s = .528 \pm 0.010\ ft^2$ (20 to 1)

$$\frac{\omega_h}{h} = .027$$

$$h = 18.2 \pm .5 \text{ BTU/hr-ft}^2\text{-}^\circ\text{F} \qquad \text{(20 to 1)}$$

This result does not take into account the uncertainty in angular location in this region. This uncertainty is estimated to be ± 3 degrees (20 to 1).

The uncertainty in the total heat transfer coefficient remained relatively constant around the entire circumference of the cylinder. However, the uncertainty in angular location varied from a maximum of ± 5 degrees (20 to 1) in the stagnation region and the wake region to a minimum of ± 1 degree (20 to 1) in the regions near the laminar separation point and the reattachment point.

RADIATIVE HEAT TRANSFER COEFFICIENT, h_r

The radiative heat transfer coefficient was determined from the equation

$$h_r = \sigma F_{1-2}(T + T_\infty)(T^2 + T_\infty^2)$$

Assuming the uncertainty in the temperature measurement is the same for both T and T_∞, and defining $T_m = \frac{1}{2}(T + T_\infty)$,

$$h_r = 4\sigma F_{1-2} T_m^3$$

Since σ is a universal constant, it does not enter into the uncertainty. Therefore,

$$\frac{\omega_{h_r}}{h_r} = \sqrt{\left(\frac{\omega_{F_{1-2}}}{F_{1-2}}\right)^2 + \left(\frac{3\omega_{T_m}}{T_m}\right)^2}$$

The radiation exchange factor, F_{1-2}, can be shown to be equal to the emissivity of the Temsheet. Since this value was not known, a value of

0.9 was chosen based upon the emissivities of comparable materials. The uncertainty in this value was assumed to be ± .05 (20 to 1). Hence, at a Reynolds number of 153,520 and an angular location of 330 degrees

$$\frac{\omega_{h_r}}{h_r} = 0.06$$

$$h_r = 1.04 \pm 0.06 \text{ BTU/hr-ft}^2\text{-}^\circ\text{F} \qquad \text{(20 to 1)}$$

NUSSELT NUMBER, Nu

The Nusselt number was calculated from the equation

$$Nu = h_c D/k = (h-h_r)D/k$$

Therefore

$$\frac{\omega_{Nu}}{Nu} = \sqrt{\left(\frac{\omega_h}{h}\right)^2 + \left(\frac{\omega_{h_r}}{h_r}\right)^2 + \left(\frac{\omega_D}{D}\right)^2 + \left(\frac{\omega_k}{k}\right)^2}$$

Since the uncertainties in the properties of air were considered neglible and the uncertainty in the diameter measurement was negliglibly small,

$$\frac{\omega_{Nu}}{Nu} = \sqrt{\left(\frac{\omega_h}{h}\right)^2 + \left(\frac{\omega_{h_r}}{h_r}\right)^2}$$

$$\frac{\omega_{Nu}}{Nu} = .029$$

$$Nu = 378 \pm 11 \qquad \text{(20 to 1)}$$

REYNOLDS NUMBER, Re

The Reynolds number was calculated from the equation

$$Re = U_\infty D/\nu$$

Therefore,

$$\frac{\omega_{Re}}{Re} = \sqrt{\left(\frac{\omega_{U_\infty}}{U_\infty}\right)^2 + \left(\frac{\omega_D}{D}\right)^2 + \left(\frac{\omega_\nu}{\nu}\right)^2}$$

The quantity U_∞ is directly proportional to the square root of the wind tunnel micromanometer reading ΔH; hence

$$\frac{\omega_{U_\infty}}{U_\infty} = 0.5 \frac{\omega_{\Delta H}}{\Delta H}$$

Again, since the uncertainty in the kinematic viscosity and in the cylinder are negligible,

$$\frac{\omega_{Re}}{Re} = 0.5 \frac{\omega_{\Delta H}}{\Delta H}$$

At a Reynolds number of 153,520 (ΔH = 3.58 cm. H_2O) the uncertainty in the micromanometer reading was estimated to be ± 0.03 cm. H_2O. Hence,

$$\frac{\omega_{Re}}{Re} = 0.5(0.03/3.58)$$

$$\frac{\omega_{Re}}{Re} = 0.004$$

Therefore,

$$Re = 153{,}520 \pm 614 \qquad (20 \text{ to } 1)$$

PRESSURE COEFFICIENT, C_p

The pressure coefficient was determined from the equation

$$C_p = \frac{P_\theta - P_s}{P_{pc} - P_s} = \frac{\Delta P_\theta}{\Delta P_{pc}}$$

Therefore,

$$\frac{\omega_{C_p}}{C_p} = \sqrt{\left(\frac{\omega_{\Delta P_\theta}}{\Delta P_\theta}\right)^2 + \left(\frac{\omega_{\Delta P_{pc}}}{\Delta P_{pc}}\right)^2}$$

Since both the pressure differences were measured on the same manometer bank, they shared the same uncertainty which was considered to be ± 0.05 in. H_2O (20 to 1). Therefore, at a Reynolds number of 156,180 and an angular location of 90 degrees,

$$\frac{\omega_{C_p}}{C_p} = 0.022$$

$$C_p = -2.14 \pm 0.05 \qquad \text{(20 to 1)}$$

LIST OF REFERENCES

1. Wirzburger, A. H., An Environmental Heat Transfer Study of a Rocket Motor Storage Container System, MSME Thesis, Naval Postgraduate School, 1972.

2. Field, R. J., Liquid Crystal Mapping of the Surface Temperature on a Heated Cylinder Placed in a Crossflow of Air, MSME Thesis, Naval Postgraduate School, 1974.

3. Meyer, J. F., An Experimental Investigation of the Heat Transfer Characteristics of a Heated Cylinder Placed in a Crossflow of Air, ENGR Thesis, Naval Postgraduate School, 1973.

4. Goldstein, R. J., Eriksen, V. L., Olsen, R. M., and Eckert, E. R. G., "Laminar Separation, Reattachment, and Transition of the Flow Over a Downstream-Facing Step," Journal of Basic Engineering, v. , p. 732-741, December 1970.

5. Abbott, D. E. and Kline, S. J., "Experimental Investigation of Subsonic Turbulent Flow Over Single and Double Backward Facing Steps," Journal of Basic Engineering, v. 84, p. 317-325, September 1962.

6. Moore, T. W. F., "Some Experiments on the Reattachment of a Laminar Boundary Layer Separating from a Rearward Facing Step on a Flat Plate Airfoil," Journal of the Royal Aeronautical Society, v. 64, p. 668-672, November 1960.

7. Grove, A. S., Shair, F. H., Petersen, E. E., and Acrivos, A., "An Experimental Investigation of the Steady Separated Flow Past a Circular Cylinder," Journal of Fluid Mechanics, v. 19, p. 60-80, May 1964.

8. National Advisory Committee for Aeronautics Report 1356, Investigation of Separated Flows in Supersonic and Subsonic Streams With Emphasis on the Effect of Transition, by D. R. Chapman, D. M. Kuehn, and H. K. Larson, 1958.

9. Lighthill, M. J., "On Boundary Layers and Upstream Influence. Part I: A Comparison Between Subsonic and Supersonic Flows," Proceedings of the Royal Society, v. 217, p. 344-348, 1953.

10. Luzhanskiy, B. Y. E. and Solntsev, V. P., "Experimental Study of Heat Transfer in the Zone of Turbulent Boundary Separation Ahead of a 'Step'," Heat Transfer-Soviet Research, v. 3, no. 6, p. 200-206, November-December 1971.

11. Chilcott, R. E., "A Review of Separated and Reattaching Flows with Heat Transfer," International Journal of Heat and Mass Transfer, v. 10, p. 783-797, 1967.

12. Larson, H. K., "Heat Transfer in Separated Flows," Journal of Aero/Space Sciences, v. 26, p. 731, 1959.

13. Seban, R. A., Emery, A., and Levy, A., "Heat Transfer to Separated and Reattached Subsonic Turbulent Flows Obtained Downstream of a Surface Step," Journal of Aero/Space Sciences, v. 26, p. 809-814, 1959.

14. Seban, R. A., "Heat Transfer to the Turbulent Separated Flow Downstream of a Step in the Surface of a Plate," Journal of Heat Transfer, v. 88, p. 276-284, 1964.

15. Filetti, E. G. and Kays, W. M., "Heat Transfer in Separated, Reattached, and Redeveloped Regions Behind a Double Step at Entrance to a Flat Duct," Journal of Heat Transfer, v. 84, p. 163-168, May 1967.

16. Charwat, A. F., Roos, J. N., Dewey, F. C., and Hitz, J. A., "An Investigation of Separated Flows. Part I: The Pressure Field," Journal of Aero/Space Sciences, v. 28, p. 457-466, 1961.

17. Vasilu, J., "Pressure Distribution in Regions of Stepwise Induced Turbulent Separation," Journal of Aero/Space Sciences, v. 29, p. 596-599, 1962.

18. Kline, S. J. and McClintock, F. A., "Describing Uncertainties in Single-Sample Experiments," Mechanical Engineering, v. 75, p. 3-8, January 1953.

INITIAL DISTRIBUTION LIST

		No. Copies
1.	Defense Documentation Center Cameron Station Alexandria, Virginia 22314	2
2.	Library, Code 0212 Naval Postgraduate School Monterey, California 93940	2
3.	Department Chairman, Code 59 Department of Mechanical Engineering Naval Postgraduate School Monterey, California 93940	1
4.	T. E. Cooper, Code 59cg Department of Mechanical Engineering Naval Postgraduate School Monterey, California 93940	3
5.	LT Jon P. McComas NROTC Unit, UCLA Los Angeles, California 90024	1
6.	C. F. Markarian Code 4061 Naval Weapons Center China Lake, California 93555	1